On Temporal-Constraint Subgraph Matching

Xiaoyu Leng†, Guang Zeng‡, Hongchao Qin†, Longlong Lin#, Rong-Hua Li†
†*Beijing Institute of Technology, China;* ‡*Ant Group;* #*Southwest University, China*
xiaoyuleng@bit.edu.cn; zengguang_77@qq.com; hcqin@bit.edu.cn; longlonglin@swu.edu.cn; rhli@bit.edu.cn

***Abstract*—Temporal-constraint subgraph matching has emerged as a significant challenge in the study of temporal graphs, which model dynamic relationships across various domains, such as social networks and transaction networks. However, the problem of temporal-constraint subgraph matching is NP-hard. Furthermore, because each *temporal-constraint* contains a permutation of temporal parameters, existing subgraph matching acceleration techniques demonstrate limited applicability to temporal-constrained graphs. Traditional continuous subgraph matching approaches prove inadequate in addressing this complex problem due to their inability to effectively handle temporal constraints. This paper addresses the challenge of identifying subgraphs that not only structurally align with a given query graph but also satisfy specific temporal-constraints on the edges. We introduce three novel algorithms to tackle this issue: the TCSM-V2V algorithm, which uses a vertex-to-vertex expansion strategy and effectively prunes non-matching vertices by integrating both query and temporal-constraints into a temporal-constraint query graph; the TCSM-E2E algorithm, which employs an edge-to-edge expansion strategy, significantly reducing matching time by minimizing vertex permutation processes; and the TCSM-EVE algorithm, which combines edge-vertex-edge expansion to eliminate duplicate matches by avoiding both vertex and edge permutations. Notably, our optimal TCSM-EVE algorithm achieves an average three-order-of-magnitude speedup on large-scale datasets. Extensive experiments conducted across 6 datasets demonstrate that our approach outperforms existing methods in terms of both accuracy and computational efficiency.**

I. Introduction

Subgraph matching is a fundamental problem in graph theory. Given a data graph d and a query graph q, the objective is to identify all subgraphs of d that are isomorphic to q. While most recent studies focus on subgraph matching in static graphs [1]–[9] or continuous subgraph matching [10]–[16], real-world graphs are often enriched with temporal information. The following scenarios illustrate the critical role of temporal subgraph matching in practical applications.

- In the financial sector, account transfers can be represented as a temporal graph, where accounts are modeled as vertices and transactions as time-stamped edges. Money laundering schemes often manifest through complex transaction patterns distributed over time [17]–[19]. Detecting such activities necessitates the identification of suspicious subgraphs.
- In telecommunication networks, call and message logs generates temporal graphs, where users as vertices and communications as timestamped edges. Analyzing these interactions can reveal patterns such as frequent bursts or specific sequences of messages. Identifying such temporal subgraphs is essential for detecting fraudulent activities, including scam operations and coordinated attacks [20]–[22].

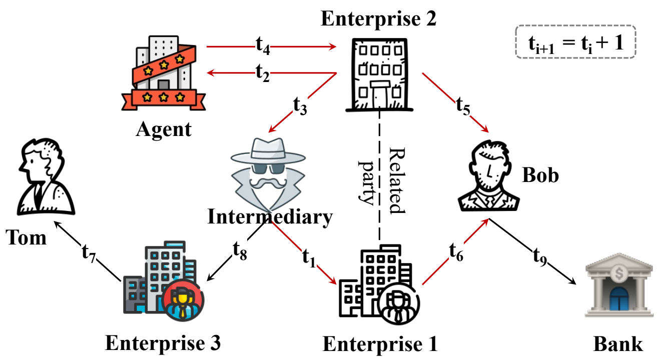

Fig. 1: A temporal bill circulation network in Ant Group.

A specific example is illustrated in Figure 1, depicting a financial bill circulation network frequently observed in Ant Group's data. In this network, each vertex represents an entity such as an enterprise, bank, intermediary, and individual, while each edge signifies a transaction behavior between these entities. Each edge is associated with a set of timestamps indicating when these interactions occurred, with t_i $(i \in N)$ following an arithmetic sequence characterized by a common difference of one day. A significant risk within the financial bill circulation network arises from the activities of bill intermediaries. These intermediaries purchase acceptance bills from companies at a discounted price using cash, subsequently transferring the bills to other enterprises or banks to earn an interest margin. For instance, the subgraph model red highlighted in Figure 1 represents a typical risk intermediary model [17]–[19], [23]. The suspected intermediary is depicted as purchasing acceptance bills with cash and rapidly transferring them. **Unlike traditional subgraph patterns, the *temporal-constraints* within these transactions are temporally linked, which means these transactions must occur within a designated time window of Δt.** Thus, *temporal-constraint* subgraph matching enhances the accuracy of detecting risky transactions within the financial bill circulation network.

Existing TCSM methods ([20], [24], [25]) define edge temporal order and global time window constraints but often generate numerous false positives. To address this limitation, our proposed methodology introduces a dual-constraint Temporal-Constraints framework that incorporates both sequential order and temporal interval upper bounds, thereby reducing false positives and improving accuracy in detecting

TABLE I: **Notations**

Notations	Descriptions
G_q and $\mathbb{TC}$	query graph and temporal-constraints
$\mathbb{G}$	data temporal graph
$\mathcal{TCQ}$ and $\mathcal{TCQ}+$	temporal-constraint query graph
$\mathcal{TO}$ and $\mathcal{PD}$	temporal order and prec dictionary
$\mathcal{FV}(\mathcal{E})$ and $\mathcal{TC}$	forward vertex (edge) and time constraint
$d.in(u)$, $d.out(u)$	in-degree and out-degree of u
$L(u)$ and $N(u)$	label and neighbors of u

financial fraud patterns with varying urgency and intervals. Given the critical importance of matching subgraphs with *temporal constraints* across various applications, our research focuses on *temporal-constraint subgraph matching* (TCSM). However, subgraph matching is an NP-hard problem, and consequently, the *TCSM* problem is also NP-hard (as demonstrated in Section 2). To enhance the efficiency of subgraph matching and continuous subgraph matching, researchers have proposed various advanced techniques. Despite the NP-hard nature of the problem, these techniques can achieve subgraph matching within graphs containing millions of vertices in milliseconds [1], [2], [5], [10]–[12], [26]. However, they face significant challenges in accelerating the *TCSM* problem. As a result, **non-optimized techniques may require up to kilo-seconds to match a temporal-constraint subgraph within a large temporal graph. This inefficiency arises because the matching process involves time-consuming permutations of vertices and edges after each match to validate the temporal constraints.**

To tackle this challenge, we designed efficient algorithms for the *TCSM* problem and conducted extensive experiments to validate their effectiveness. The contributions are as follows:

- We introduce the TCSM-V2V algorithm, which performs vertex expansion in a vertex-to-vertex manner. This algorithm merges the query and temporal-constraints graphs into a *Temporal-Constraint Query Graph* ($\mathcal{TCQ}$), which leverages temporal-constraints to prune final vertices and reduces unnecessary duplicate matches.
- We present the TCSM-E2E algorithm, which utilizes an edge-to-edge expansion approach. This algorithm integrates the query graph and *temporal constraints* graph into the $\mathcal{TCQ}+$ graph. By minimizing the vertex permutation process inherent in the TCSM-V2V algorithm, this method significantly reduces the matching time.
- We propose the TCSM-EVE algorithm, which employs an interactive edge-vertex-edge expansion strategy. This approach produces results **without the need for vertex and edge permutations**, minimizing duplicate matches.
- Experiments on 7 real-world temporal datasets demonstrate that our TCSM-EVE algorithm consistently outperforms other algorithms in nearly all scenarios. For instance, while the baseline RI-DS algorithm takes 4071.4 seconds to match query q_1 with temporal constraint tc_2 on the WT dataset, TCSM-EVE **completes the task in just 2.5 seconds**.
- The code is available at https://github.com/xiaoyu-ll/TSI.

II. Preliminaries

In this section, we first introduce several fundamental concepts. A simple directed graph can be represented by $G = (V, E, \mathcal{L})$, where V is a set of vertices, E is a set of edges where each edge is a pair (u, v) and $u, v \in V$, and $\mathcal{L}$ is a label function that maps the vertex $u \in V$ to a label $\mathcal{L}(u)$. Note that, we only consider graphs with labeled vertices. However, if edges are also labeled, the algorithm can be easily generalized. Given a query graph $G_q = (V_q, E_q, \mathcal{L}_q)$ and a data graph $G = (V, E, \mathcal{L})$, a subgraph matching (isomorphism) is an injective function $f : V_q \rightarrow V$ that satisfies: $\forall u \in V_q$, $\mathcal{L}_q(u) = \mathcal{L}(f(u))$; and $\forall(u,v) \in E_q$, $(f(u), f(v)) \in E$.

In this paper, we focus on the problem of matching the subgraphs with *temporal constraints* in the temporal graph. We define the data temporal graph, the query graph, and the *temporal-constraint* graph as follows.

Definition 1 (Data Temporal Graph ($\mathbb{G}$)): A simple directed data temporal graph can be represented by $\mathbb{G} = (\mathcal{V}, \mathcal{E}, \mathcal{L}, \mathcal{T})$, where $\mathcal{V}$ is the set of vertices; $\mathcal{E}$ is a set of *temporal edges* where each *temporal edge* is (u, v, t), $u, v \in V$ and $t \in \mathcal{T}$ denotes the interaction time between u and v; $\mathcal{L}$ is a label function that maps the vertex $u \in V$ to a label $\mathcal{L}(u)$; $\mathcal{T}$ is a set of all the timestamps.

By Definition 1, we use $\mathcal{T}(u, v)$ to stand for the set of timestamps in which u and v and interacted, and $e.t$ to represent the interaction time of the edge $e \in \mathcal{E}$ in the temporal graph. For a temporal graph $\mathbb{G}$, the *de-temporal graph* of $\mathcal{G}$ denoted by $G = (V, E)$ is a graph that ignores all the timestamps associated with the temporal edges. More formally, for the de-temporal graph G of $\mathcal{G}$, we have $V = \mathcal{V}$ and $E = \{(u, v) | (u, v, t) \in \mathcal{E}\}$.

Definition 2 (Query Graph (G_q)): A query graph $G_q = (V_q, E_q, \mathcal{L}_q)$ is a labeled simple directed graph.

Assuming that set E_q in G_q adheres to a specific order $\{e_1, e_2 ... e_{|\mathcal{E}|}\}$, we define the *temporal-constraint* graph that adheres to the temporal constraints as follows.

Definition 3 (Temporal-Constraints ($\mathbb{TC}$)): The temporal-constraint $\mathbb{TC}$ is a set of triples, in which each triple (i, j, k) represents that the interaction time of e_j minus the interaction time of e_i is not larger than k, i.e. $0 \leq e_j.t - e_i.t \leq k$.

Based on Definition 3, we can observe that the $\mathbb{TC}$ is a simple directed edge-weighted graph. This implies the absence of loops and the exclusion of multiple edges within the graph's architecture, as illustrated in Figure 2(b). Moving forward, we present a formal definition of the problem, which involves the subgraph isomorphism considering *temporal constraints* on a temporal graph.

Definition 4 (Temporal-Constraint Subgraph Matching): Given a query graph $G_q = (V_q, E_q, \mathcal{L}_q)$, the temporal-constraints $\mathbb{TC} = \{(i, j, k)\}$ and a data temporal graph $\mathbb{G} = (\mathcal{V}, \mathcal{E}, \mathcal{L}, \mathcal{T})$, a *temporal-constraint subgraph matching* (abbreviated as *TCSM*) from G_q to $\mathbb{G}$ under the temporal-constraint $\mathbb{TC}$ is an injective function $f : E_q \rightarrow \mathcal{E}$ which satisfies:

1) Isomorphism: $\forall(u_q, v_q) \in E_q, \exists(u, v, t) \in \mathcal{E} \rightarrow f((u_q, v_q)) = (u, v, t), \mathcal{L}_q(u_q) = \mathcal{L}(u), \mathcal{L}_q(v_q) = \mathcal{L}(v)$.

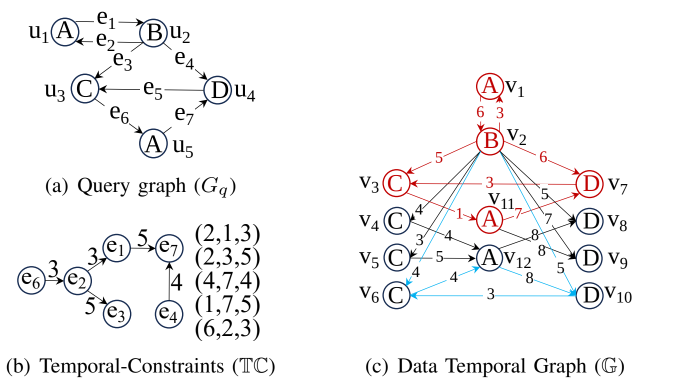

(a) Query graph (G_q)

(b) Temporal-Constraints ($\mathbb{TC}$)

(c) Data Temporal Graph ($\mathbb{G}$)

Fig. 2: A toy example.

2) Temporal-constraint: Consider E_q=$\{e_1, e_2 ... e_{|E_q|}\}$, $\forall(i,j,k) \in \mathbb{TC} \rightarrow 0 \leq f(e_j).t - f(e_i).t \leq k$.

Problem of TCSM: Given a query graph G_q, the temporal-constraints $\mathbb{TC}$, and a data temporal graph $\mathbb{G}$, our task is to find all the subgraph matchings from G_q to $\mathbb{G}$ under $\mathbb{TC}$.

Example 1: Figure 2(a-c) show a toy example for query graph G_q, temporal-constraints $\mathbb{TC}$ and data temporal graph $\mathbb{G}$. Figure 2(a) shows that G_q contains 5 vertices and 7 directed edges, and each vertex in G_q has a label ($\mathcal{L}_q(u_1, u_5)$=A; $\mathcal{L}_q(u_2)$=B; ...). Figure 2(b) indicates that $\mathbb{TC}$ has 5 items ($0 \leq e_1.t - e_2.t \leq 3; 0 \leq e_3.t - e_2.t \leq 5;...$), which can be assembled into a form of graph. In Figure 2(c), each vertices has a label, and each edge has a timestamp ((v_1, v_2).t=6; (v_2, v_1).t=3; ...). A *TCSM* from G_q to $\mathbb{G}$ under $\mathbb{TC}$ is highlighted in red, which is the matching $\{u_1, u_2, u_3, u_4, u_5 \rightarrow v_1, v_2, v_3, v_7, v_{11}\}$. We can observe that their labels are matching ($\mathcal{L}_q(u_1, u_5)$=A=$\mathcal{L}(v_1, v_{11})$; ...), and the temporal-constraints are satisfied ($e_1 \rightarrow (v_1, v_2), e_2 \rightarrow (v_2, v_1), 0 \leq (v_1, v_2).t - (v_2, v_1).t$=$3 \leq 3$;...). However, if temporal information is disregarded, the subgraph marked in blue can be a traditional subgraph matching from G_q to G since their labels are matching, and it is not a *TCSM* since $e_2 \rightarrow (v_2, v_1), e_6 \rightarrow (v_6, v_{12}), (v_2, v_1).t - (v_6, v_{12}).t$=$-1$, conflict to $0 \leq e_2.t - e_6.t \leq 3$.

Theorem 1 (NP-hardness of TCSM): The Temporal-Constraint Subgraph Matching problem is NP-hard.

The proof of Theorem 1 can be established by considering a special case: if the time constraint k in each triplet of the temporal constraint is set to infinity, the Subgraph Matching problem can be reduced to the *TCSM* problem. Since Subgraph Matching is a well-known NP-hard problem, this reduction demonstrates the validity of the theorem.

Challenges: As noted, the *TCSM* problem is NP-hard. Traditional Subgraph Matching methods use filtering, verification, optimized matching order, and indexing (see Section 6), but these face challenges in the *TCSM* context. **First**, the temporal aspect adds complexities beyond static matching, requiring structural matches in temporal graphs while satisfying temporal constraints. **Second**, temporal constraints affect the matching order, increasing computational burden due to combinatorial factors. **Third**, using decomposition and indexing leads to unmanageable index sizes due to the added complexity of matching order. In summary, existing optimization techniques are not directly applicable to the *TCSM* problem.

III. Basic Algorithm for TCSM

We propose an algorithm for $TCSM$ with vertex expansion in a Vertex-To-Vertex manner, abbreviated as TCSM-V2V. Before introducing the specific details of the algorithm, we need to consider the following key observations.

O1. Matching Orders. Traditional methods prioritize matching orders based on high-degree vertices, small candidate sets and the structure of query graph. In $TCSM$, the matching order must also consider the *temporal-constraint*.

O2. Candidates Filtering. Filtering methods based on neighboring vertices, labels, and degrees are widely used to reduce the candidate data vertices. However, these methods often result in excessive candidates. Therefore, a more effective approach is needed to further minimize the candidates.

O3. Validity Checking. It is necessary to employ certain methods to determine whether a candidate data vertex can match a query vertex. This can be done by checking the edges between the query vertex and its matched neighbors, or by using matrix calculations with the state space method. However, both approaches are computationally demanding, with the latter being more suitable for smaller data graphs. Our goal is to develop a less resource-intensive and faster pruning method for validating candidate data vertices.

O4. Temporal-Constraint Checking. Our solution needs to find all subgraphs in the data graph that satisfy both the query and the *temporal-constraint* graph. This requires the algorithm to continuously check partial matches against both graphs.

Building on the four observations, we introduce the concept of a *temporal-constraint query graph*, denoted as $\mathcal{TCQ}$. The $\mathcal{TCQ}$ encompasses not only the structural information of the query graph and the temporal information of *temporal-constraint* graph but also the matching order of the vertices and the method by which each vertex candidate set is generated.

A. The construction of $\mathcal{TCQ}$

The $\mathcal{TCQ}$ is formed by four hash tables Temporal Order $\mathcal{TO}$, Prec Dictionary $\mathcal{PD}$, Forward Vertex $\mathcal{FV}$, and Time Constraint $\mathcal{TC}$. As shown in Figure 3, the vertices are aligned from left to right, indicating the order of the matching query vertices. For two vertices connected by a solid line, the preceding vertex is the *prec* (predecessor) of the subsequent one. For vertices connected by a dotted line, the preceding vertex is a member of the *forward vertex* of the latter vertex. The direction of the arrows shows the direction of the corresponding edges between the vertices in the query graph. The positions labeled tc_1 to tc_5 indicate where time-based pruning should be applied for each *temporal constraint*. The entire construction process is summarized in Algorithm 1 (details are below).

Algorithm 1: $\mathcal{TCQ}(G_q, \mathbb{TC}, \mathbb{G})$

```
   input : $G_q$, $\mathbb{TC}$ and $\mathbb{G}$.
   output: four hash tables $\mathcal{TO}$, $\mathcal{PD}$, $\mathcal{FV}$, $\mathcal{TC}$ of $\mathcal{TCQ}$.
   // compute tsup for each query vertex
1  for each $u \in V_q$ do $tsup[u] = 0$;
2  for each $tc = (i, j, k) \in \mathbb{TC}$ do
3      $tsup[e_i.u]$++; $tsup[e_i.v]$++; $tsup[e_j.u]$++; $tsup[e_j.v]$++;
4  $\mathcal{TO}[1] \leftarrow \arg\max_{u \in V_q}\{tsup[u]\}$;
5  $\mu \leftarrow 2$;
6  while $\mu \leq |V_q|$ do
7      $V_q^\mu = \{u | u \in V_q \& u \notin \mathcal{TO}\}$, $N_\mu(u) = \{v | v \in \mathcal{TO} \& (u, v) \in E_q\}$;
8      $\mathcal{TO}[\mu] \leftarrow \arg\max_{u \in V_q^\mu}\{|N_\mu(u)|\}$;
9      $\mathcal{PD}[\mu] = \arg\min_{u \in N_\mu(\mathcal{TO}[\mu])}\{\mathcal{TO}'[u]\}$;
10     $\mathcal{FV}(\mu) \leftarrow N_\mu(\mathcal{TO}[\mu]) \setminus \mathcal{PD}[\mu]$;
11     $\mu$ ++;
12 for each $tc = (i, j, k) \in \mathbb{TC}$ do
13     $\mathcal{TC}[tc] = \arg\max_{u \in \{e_i.u, e_i.v, e_j.u, e_j.v\}}\{\mathcal{TO}'[u]\}$;
14 return ($\mathcal{TO}$, $\mathcal{PD}$, $\mathcal{FV}$, $\mathcal{TC}$);
```

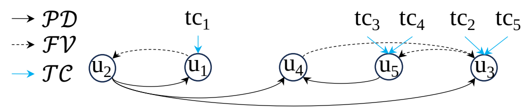

$\mathcal{TO}$ ={1:u_2, 2:u_1, 3:u_4, 4:u_5, 5:u_3} $\mathcal{FV}$ ={u_1:{u_2}, u_4:∅, u_5: ∅, u_3:{u_4,u_5}}
$\mathcal{PD}$ ={u_1:u_2, u_4: u_2, u_5:u_4, u_3:u_2} $\mathcal{TC}$ ={tc_1:u_1, tc_2:u_3, tc_3:u_5, tc_4:u_5, tc_5:u_3}

Fig. 3: Temporal-Constraint Query Graph $\mathcal{TCQ}$.

In the following, we show how to construct the four attached hash tables $\mathcal{TO}$, $\mathcal{PD}$, $\mathcal{FV}$, and $\mathcal{TC}$.

Definition 5 (Temporal-Constraint Support (tsup)): Given a query graph $G_q = (V_q, E_q, \mathcal{L}_q)$ and the *temporal constraints* graph, the *Temporal-Constraint Support* of a vertex $u \in V_q$ is the sum of the degrees of edges that contain u within the temporal constraint graph, i.e., $tsup(u) = \sum_{i=1}^{|E_q|} d(e_i), u \in e_i$.

Temporal Order. The vertex ordering method is based on *tsup*, prioritizing query vertices that have the highest support and strongest connections with vertices already in $\mathcal{TO}$. First, *tsup* is calculated for each query vertex (Algorithm 1, Lines 1-3). The vertex with the highest *tsup* is selected as the starting vertex (Algorithm 1, Line 4). In case of a tie, the vertex with the fewest candidates is chosen; if the tie persists, selection is made randomly. Subsequent vertices are chosen based on their connections to vertices in $\mathcal{TO}$ (Algorithm 1, Lines 7-8).

Prec Dictionary. In the context of $\mathcal{TO}$, a query vertex is developed from another query vertex. Specifically, the latter becomes a candidate of $\mathcal{TCQ}$ because of the former, with the former referred to as the *prec* of the latter. The *Prec Dictionary* ($\mathcal{PD}$) stores the predecessor of each query vertex (Algorithm 1, Line 9). Beyond the initial vertex, candidate data vertices for matching are generated based on the partially matched subgraph. Since the $\mathcal{TCQ}$ graph stores structural relationships between vertices and their *prec*, candidate data vertices can be identified from the neighbors of already-matched predecessors. This approach reduces the size of candidate sets compared to other traditional candidate filtering methods.

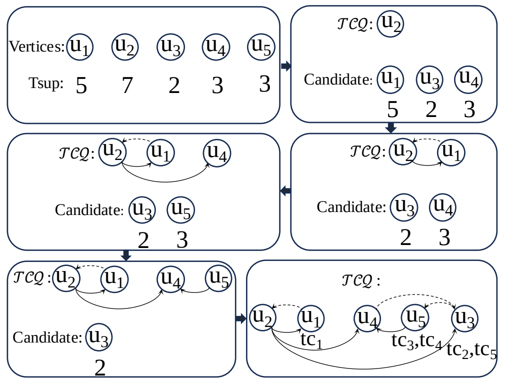

Vertices:
u_1 u_2 u_3 u_4 u_5
Tsup: 5 7 2 3 3
$\mathcal{TCQ}$: u_2
Candidate: u_1 u_3 u_4
5 2 3
$\mathcal{TCQ}$: u_2 u_1
Candidate: u_3 u_4
2 3
$\mathcal{TCQ}$: u_2 u_1 u_4
Candidate: u_3 u_5
2 3
$\mathcal{TCQ}$: u_2 u_1 u_4 u_5
Candidate: u_3
2
$\mathcal{TCQ}$:
u_2 u_1 u_4 u_5 u_3
tc_1
tc_3,tc_4
tc_2,tc_5

Fig. 4: The construction of $\mathcal{TCQ}$.

Forward Vertex. To maintain the integrity of the query graph structure, *Forward Vertex* is created to track the neighboring vertices that already in $\mathcal{TCQ}$, excluding the *prec* (Algorithm 1, Line 10). This approach efficiently captures the structural relationships in the query graph while ensuring the accuracy of matched data vertices. When determining whether a data vertex can match a query vertex, it is essential to verify the presence of a corresponding data edge between the matched data vertex (the match of this query vertex's *forward vertex*) and this data vertex. If the edge does not exist, the data vertex cannot be considered a match for the query vertex.

Time Constraint. Once all query vertices within a *temporal constraint* have been matched, it's crucial to ensure that the current partial match adheres to the *temporal constraint*. To achieve this, $\mathcal{TC}$ is created to record the vertex that appears last in $\mathcal{TCQ}$ for each *temporal constraint*. (Algorithm 1, Lines 12-13). When determining whether a data vertex can match a query vertex, the temporal constraint must also be validated. If the current partial matching fails to satisfy the temporal constraints, then the data vertex cannot match the query vertex.

Theorem 2 (Complexity of building $\mathcal{TCQ}$): The time and space complexity of building the $\mathcal{TCQ}$ graph is $O(|V_q|^2 + |V_q| \cdot d_{\max} + |\mathcal{TC}|)$ and $O(|V_q| + |\mathcal{TC}|)$, respectively.

Proof of THEOREM 2: Initializing $tsup[u]$ for each $u \in V_q$ takes $O(|V_q|)$. Iterating over each temporal-constraint $tc \in \mathbb{TC}$ and updating $tsup$ takes $O(|\mathcal{TC}|)$. Finding the vertex with the maximum $tsup[u]$ takes $O(|V_q|)$. The main loop, which runs $|V_q| - 1$ times, involves constructing V_q^μ and finding the vertex with the maximum $|N_\mu(u)|$, each taking $O(|V_q|)$ per iteration. Additionally, finding the minimum in $N_\mu(\mathcal{TO}[\mu])$ takes $O(d_{\max})$ per iteration. Thus, the main loop has a time complexity of $O(|V_q|^2 + |V_q| \cdot d_{\max})$. Post-processing each $tc \in \mathbb{TC}$ takes $O(|\mathcal{TC}|)$ Therefore, the total time complexity is $O(|V_q|^2 + |V_q| \cdot d_{\max} + |\mathcal{TC}|)$.

The array $tsup$, hash tables $\mathcal{TO}$, $\mathcal{PD}$ and $\mathcal{FV}$ each require $O(|V_q|)$ space. Besides, the hash table $\mathcal{TC}$ require O($|\mathcal{TC}|$). Hence, the total space complexity is $O(|V_q| + |\mathcal{TC}|)$.

Example 2: Figure 4 shows the process of constructing $\mathcal{TCQ}$. The first step is to calculate the $tsup$ for each vertex to build the $\mathcal{TO}$ (recall Figure 2(b), $tsup(u_1)$=$d(e_1)$ +

$d(e_2)$=5; $tsup(u_2)$=$d(e_1)+d(e_2)+d(e_3)+d(e_4)$=7; ...). Then, we choose the vertex u_2 with the highest $tsup$, and its neighboring vertices (u_1, u_3, u_4). Next, we choose the neighbor u_1 with the highest $tsup$, and build the solid line from u_2 to u_1 (which is stored in $\mathcal{PD}$), the dashed line from u_1 to u_2 (which is stored in $\mathcal{FV}$). Subsequently, we re-compute the neighboring vertices of u_2 and u_1, but the candidate are still u_3 and u_4. u_4 is added into the $\mathcal{TCQ}$, and (u_2, u_4) is added into $\mathcal{PD}$. Next, we re-compute the neighboring vertices and the candidate vertices become u_3 and u_5, u_5 is added into the $\mathcal{TCQ}$ and this process is iterated for the remaining vertices. In the final step, we build the $\mathcal{TC}$ to record the last appears in $\mathcal{TCQ}$ for all the vertices in each *temporal constraints*. ($\mathbb{TC}_1 = (2,1,3) \rightarrow e_2, e_1 \rightarrow u_2, u_1 \rightarrow \mathcal{TC}(tc_1) = u_1$; $\mathbb{TC}_2 = (2,3,5) \rightarrow e_2, e_3 \rightarrow u_1, u_2, u_3 \rightarrow \mathcal{TC}(tc_2) = u_3$; ...).

B. *Algorithm* TCSM-V2V.

Given a temporal-constraint $\mathbb{TC}$, a query graph G_q and a data temporal graph $\mathbb{G}$, TCSM-V2V recursively expands partial matches by mapping query vertices to their respective candidates in accordance with $\mathcal{TO}$, and evaluates their structural and temporal information to determine whether they satisfy $\mathcal{FV}$ and $\mathcal{TC}$. The first step involves generating the initial candidates for each query vertex. This process aims to identify all potential data vertices while minimizing the candidate set. Inspired by the Neighborhood Label Frequency filtering technique [27], we introduce the *neighbor label filter* to effectively filter data vertices for each query vertex.

Definition 6 (Neighbor Label Filter (NLF)*):* Given a query graph $G_q = (V_q, E_q, \mathcal{L}_q)$ and a data temporal graph $\mathbb{G} = (\mathcal{V}, \mathcal{E}, \mathcal{L}, \mathcal{T})$ and the *de-temporal graph* $G = (V, E)$ of $\mathbb{G}$. Given $u \in V_q$ and $v \in V$, a *neighbor label filter* (v, u) is an injective function m: $v \rightarrow u$ that satisfies:

1) $L(v) = L(u)$.
2) $d.in(v) \geq d.in(u)$, $d.out(v) \geq d.out(u)$.
3) $\forall\ u' \in N(u)$, $\exists\ v' \in N(v)$, $L(v') = L(u')$.

Algorithm 2 presents our TCSM-V2V algorithm, which take $\mathbb{TC}$, G_q and $\mathbb{G}$ as input, and outputs all *temporal-constraint subgraph matchings* M from G_q to $\mathbb{G}$ under $\mathbb{TC}$. We first find all the possible initial candidates in $\mathbb{G}$ for each query vertex (Lines 1-3). Next, we generate $\mathcal{TO}$, $\mathcal{PD}$, $\mathcal{FV}$, and $\mathcal{TC}$ (Line 4). Then, we start the matching process by expanding the partial match in vertex-to-vertex manner recursively following $\mathcal{TO}$ (Lines 5-8). If all query vertices have been matched, we output the result (Lines 10-11). Otherwise, we obtain the next query vertex u in $\mathcal{TO}$, the *prec* of u and set the candidate data vertices set of u to empty (Line 13). We extract the candidates data vertices of u based on the data vertex mapped to the *prec* of u and the structural correlation between u and the *prec* of u (Lines 14-16). For each candidate data vertex v of u, Line 18 checks whether there are edges between the candidate data vertex and the data vertices matched to the neighbors of u (Lines 22-24). If the query vertex u and the already matched query vertices can form a *temporal constraint* (tc) through their connecting edges, it is necessary to evaluate whether the temporal relationships of the partial match, after

Algorithm 2: TCSM-V2V(G_q, $\mathbb{TC}$, $\mathbb{G}$)

```
   input   : $G_q$, $\mathbb{TC}$ and $\mathbb{G}$.
   output  : all TCSMs $M$ from $G_q$ to $\mathbb{G}$ under $\mathbb{TC}$.
   // generate initial candidate set (by def. 7)
1  for each $u \in V_q$ do
2      for each $v \in V$ do
3          if NLF($v, u$) is true then $u.C \leftarrow v$;
   // generate $\mathcal{TCQ}$ graph
4  ($\mathcal{TO}$,$\mathcal{PD}$,$\mathcal{FV}$,$\mathcal{TC}$) $\leftarrow$ $\mathcal{TCQ}$($\mathbb{TC}$, $G_q$, $\mathbb{G}$);
   // matching process.
5  $\lambda \leftarrow 1$, $u \leftarrow \mathcal{TO}[\lambda]$, $M \leftarrow \emptyset$;
6  for each $v \in u.C$ do
7      $M[u] \leftarrow v$;
8      DFS ($\mathbb{G}$, $\mathcal{TO}$, $\mathcal{PD}$, $\mathcal{FV}$, $\mathcal{TC}$, $M$, $\lambda$+1);
9  Procedure DFS ($\mathbb{G}$,$\mathcal{TO}$,$\mathcal{PD}$,$\mathcal{FV}$,$\mathcal{TC}$,$M$,$\lambda$):
10     if $\lambda$ = $|\mathcal{TO}|$ +1 then
11         print $M$;
12     else
13         $u \leftarrow \mathcal{TO}[\lambda]$, $u' \leftarrow \mathcal{PD}[u]$, $u.C \leftarrow \emptyset$;
           // generate candidate in current state
14         for each $u_c \in N(M[u'])$ do
15             if $L(u_c)$ = $L(u)$ then
16                 $u.C \leftarrow u_c$;
17         for each $v \in u.C$ do
18             if Validate($\mathbb{G}$, $\mathcal{TC}$, $\mathcal{FV}$, $M$, $u$, $v$, $\lambda$) is true then
19                 $M[u] \leftarrow v$;
20                 DFS ($\mathbb{G}$, $\mathcal{TO}$, $\mathcal{PD}$, $\mathcal{FV}$, $\mathcal{TC}$, $M$, $\lambda$+1);
21 Function Validate($\mathbb{G}$, $\mathcal{TC}$, $\mathcal{FV}$, $M$, $u$, $v$, $\lambda$):
22     for each $u' \in FN(u)$ do
23         if $e(M[u'], v) \notin E(\mathbb{G})$ then
24             return false;
25     for each $tc \in \mathbb{TC}$ do
26         if $M$ do not satisfy time constraint $tc$ then
27             return false;
28     return true;
```

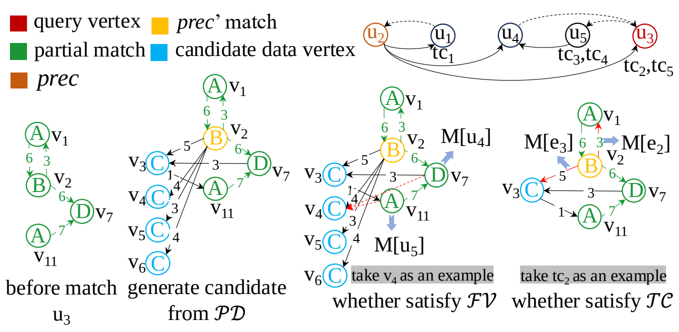

Fig. 5: A specific matching process of algorithm 2.

incorporating vertex v, satisfy the specified tc (Lines 25-27). If so, we expand the partial match by matching the next query vertex (Lines 19-20). Otherwise, the algorithm matches the next candidate vertex or backtracks to the last query vertex.

Example 3: Suppose the partial matching is $M = \{u_2 : v_2; u_1 : v_1; u_4 : v_7; u_5 : v_{11}\}$, we need to match vertex u_3. The first step involves generating candidate from $\mathcal{PD}$, so we match from the *prec* vertex of u_3 from $\mathcal{TCQ}$. The *prec* vertex is u_2 and $M(u_2) = v_2$. Among the neighbors of v_2, $\{v_3, v_4, v_5, v_6\}$ are generated , which have same label as u_3. Then, we check whether the candidate vertices satisfy

$\mathcal{FV}$. Consider $M(u_3) = v_4$, since $\mathcal{FV}[u_3]$ = $\{u_4,\ u_5\} \rightarrow v_4$ must have edge to $M(u_4) = v_7$ and $M(u_5) = v_{11}$, conflit to v_4 only has edges with v_2 and v_{12} and does not have edge with v_7 and v_{11} in Figure 2(c). So v_4 will be removed from the candidates, and v_5, v_6 will also be removed in this step. Next, we check whether the candidate vertices satisfy $\mathcal{TC}$. Consider $M(u_3) = v_3$, since $\mathcal{TC}(tc_2, tc_5)$ = u_3, $\mathbb{TC}_2, \mathbb{TC}_5 \rightarrow e_3.t - e_2.t \leq 5, e_2.t - e_6.t \leq 3$, and $e_2.t = (v_2, v_1).t = 3; e_3.t = (v_2, v_3).t = 5; e_6.t = (v_3, v_{11}).t = 1$. We can see that $0 \leq 5-3 \leq 5; 0 \leq 3-1 \leq 3$, so $M(u_3) = v_4$ is a correct matching.

Theorem 3 (Complexity of Algorithm TCSM-V2V*):* The time and space complexity of Algorithm TCSM-V2V is $O(2^{|V_q|} \times (|V| + d_{\max} + |\mathcal{TC}|))$ and $O(|V_q| + |\mathcal{TC}|)$, respectively.

Proof of THEOREM 3: The initialization (Lines 1-3) involves nested loops over $|V_q|$ and $|V|$ for checking $NLF(v, u)$, resulting in $O(|V_q| \times |V|)$. Generating the $\mathcal{TCQ}$ graph (Line 4) using the $\mathcal{TCQ}$ algorithm has a time complexity of $O(|V_q|^2 + |V_q| \cdot d_{\max} + |\mathcal{TC}|)$. The matching process (Lines 5-20), which includes initializing λ, u, and M, and performing DFS for each $v \in u.C$, involves exploring all possible subgraph matchings, leading to an exponential complexity of $O(2^{|V_q|})$. Specifically, each DFS call involves operations that take $O(|V_q| \times |V|)$ and validation steps that add $O(d_{\max})$ per edge check and $O(|\mathcal{TC}|)$ per time constraint check. Therefore, the overall time complexity is $O(2^{|V_q|} \times (|V| + d_{\max} + |\mathcal{TC}|))$.

The array $tsup$, hash tables $\mathcal{TO}$, $\mathcal{PD}$ and $\mathcal{FV}$ each require $O(|V_q|)$ space. Besides, the hash table $\mathcal{TC}$ require $O(|\mathcal{TC}|)$. The candidate set $u.C$ and the mapping M also require $O(|V_q|)$ space. Temporary variables used in loops and recursive calls consume additional $O(|V_q|)$ space. Hence, the total space complexity is $O(|V_q| + |\mathcal{TC}|)$.

Algorithm 3: $\mathcal{TCQ}$+$(G_q, \mathbb{TC}, \mathbb{G})$

```
   input : $G_q$, $\mathbb{TC}$ and $\mathbb{G}$.
   output: four hash tables $\mathcal{TO}$, $\mathcal{PD}$, $\mathcal{FE}$, $\mathcal{TC}$ of $\mathcal{TCQ}$+.
   // creat $TCF$ for temporal-constraint graph
1  $\mathscr{E} \leftarrow \emptyset$, $\mathscr{V} \leftarrow \{(N_e|e\in E_q)\}$;
2  for each $u \in V_q$ do
3      for each $e_i \in u.adje$ do
4          for each $e_j \in u.adje$ ($e_i \neq e_j$) do
5              if (i, j, k) $\in \mathbb{TC}$ then
6                  $\mathscr{E} \cup \{(N_{e_i}, N_{e_j})\}$;
7                  if $(\mathscr{V}, \mathscr{E})$ is cyclic then
8                      $\mathscr{E} \setminus \{(N_{e_i}, N_{e_j})\}$;
   // compute $tsup$ for each query edge
9  for each $e \in E_q$ do $tsup[e]$ = 0;
10 for each $tc$ = (i, j, k) $\in \mathbb{TC}$ do
11     $tsup[e_i]$++; $tsup[e_j]$++;
12 $\mu \leftarrow 2$, $\mathcal{TO} \leftarrow \emptyset$, $\delta \leftarrow 0$;
13 $\mathcal{TO}[1] \leftarrow \arg\max_{e\in E_q}\{tsup[e]\}$;
14 while $\mu \leq |E_q|$ do
15     for each $e'$, $(N_{e'}, N_{\mathcal{TO}[\mu-1]}) \in \mathscr{E}$ do $\delta \leftarrow \delta$ + 1;
16     while $\delta$ >0 do
17         $N_\mu^{\mathscr{E}} = \{e|\exists e' \in \mathcal{TO}, (e, e') \in \mathscr{E}\}$;
18         $\delta \leftarrow \delta$ - 1, $\mathcal{TO}[\mu] \leftarrow \arg\max_{e\in N_\mu^{\mathscr{E}}}\{tsup[e]\}$;
19         $N_\mu = \{e|e \in \mathcal{TO}\&e \cap \mathcal{TO}[\mu] \neq \emptyset\}$;
20         $\mathcal{PD}[\mu] = \arg\min_{e\in N_\mu}\{\mathcal{TO}'[e]\}$;
21         $\mathcal{FE}[\mu] = \{e|e \in N_\mu\&e \cap \mathcal{TO}[\mu] \neq \mathcal{PD}[\mu] \cap \mathcal{TO}[\mu]\}$;
22         for each $e'$, $(N_{e'}, N_{\mathcal{TO}[\mu]}) \in \mathscr{E}$ do $\delta \leftarrow \delta$ + 1;
23         $\mu$++;
24     $N_\mu^E = \{e|\exists e' \in \mathcal{TO}, (e, e') \in E\}$;
25     $\mathcal{TO}[\mu] \leftarrow \arg\max_{e\in N_\mu^E}\{tsup[e]\}$;
26     $N_\mu$ = $\{e|e \in \mathcal{TO}\&e \cap \mathcal{TO}[\mu] \neq \emptyset\}$;
27     $\mathcal{PD}[\mu] = \arg\min_{e\in N_\mu}\{\mathcal{TO}'[e]\}$;
28     $\mathcal{FE}[\mu] = \{e|e \in N_\mu\&e \cap \mathcal{TO}[\mu] \neq \mathcal{PD}[\mu] \cap \mathcal{TO}[\mu]\}$;
29     $\mu$++;
30 for each $tc = (i, j, k) \in \mathbb{TC}$ do $\mathcal{TC}[tc]$ = $\arg\max_{e\in\{e_i,e_j\}}\{\mathcal{TO}'[e]\}$;
31 return ($\mathcal{TO}$, $\mathcal{PD}$, $\mathcal{FE}$, $\mathcal{TC}$);
```

IV. Advanced Algorithm for TCSM

A. The construction of $\mathcal{TCQ}$+

In the previous section, we introduced a vertex-to-vertex matching approach. However, the necessity of identifying specific graph patterns with temporal constraints within temporal subgraphs leads to numerous time-consuming edge permutation checks when using vertex-based matching methods. Consequently, we are investigating an edge-based matching algorithm as an alternative. In the edge-to-edge matching method, the existing $\mathcal{TCQ}$ graph becomes inadequate, as the fundamental matching unit shifts from vertices to edges. To accommodate this transition, we propose the construction of a new graph, denoted as $\mathcal{TCQ}$+. This graph involves modifications to the Temporal Order ($\mathcal{TO}$), Precursor Dictionary ($\mathcal{PD}$), and Time Constraint ($\mathcal{TC}$), while also substituting the concept of Forward Vertex ($\mathcal{FV}$) with Forward Edge ($\mathcal{FE}$). The construction process for $\mathcal{TCQ}$+ is detailed below.

The edge-based matching order must take into account both temporal and structural constraints. Each edge to be matched should share at least a common vertex with already matched query edges in query graph, eliminating the need for post-matching connections and expediting the pruning process. By treating each edge as a vertex and connecting edges in a *temporal constraint* when they share a common vertex, we construct a Temporal-Constraint Forest (TCF). For each pair of edges within the *temporal-constraint*, if they are connected, we establish an edge between them. This forest, composed of interconnected trees, optimizes the matching process by capitalizing on the interconnected nature of edges.

We also define *temporal-constraint support (tsup)* for each query edge, which is the degrees of the edge in the *temporal constraint* graph, i.e., $tsup(e) = \sum_{i=1}^{|E_q|} d(e_i)$.

Forward Edge. To maintain the integrity of the query graph structure, we introduce the *forward edge*, is defined as a neighboring edge of e that already in $\mathcal{TO}$ and shares a common vertex with e distinct from the vertex shared between e and e's $prec$. Assuming that both two vertices of the query edge to be matched are part of the vertices in certain previously matched query edges, it is necessary to maintain the consistency of the candidate data edge's two vertices with the vertices of the data edges that correspond to these matched query edges.

Algorithm 3 outlines the construction of $\mathcal{TCQ}$+. The process begins by building the TCF (Lines 1-8). Following this,

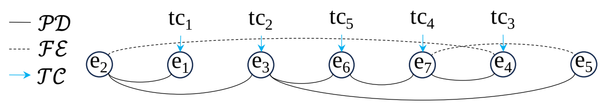

$\mathcal{TO}$ = {1:e_2, 2:e_1, 3:e_3, 4:e_6, 5:e_7 , 6:e_4, 7:e_5} $\mathcal{FE}$ = {e_1: ∅, e_3: ∅, e_6: ∅, e_7 :∅, e_4 :{e_2}, e_5 :{e_7 }}
$\mathcal{PD}$ = {e_1 :e_2, e_3 : e_2, e_6 :e_3, e_7 : e_6, e_4 :e_7, e_5 : e_3} $\mathcal{TC}$ = {tc_1 :e_1, tc_2 :e_3, tc_3 :e_4, tc_4 :e_7, tc_5 :e_6}

Fig. 6: Temporal-Constraint Query Graph $\mathcal{TCQ}+$.

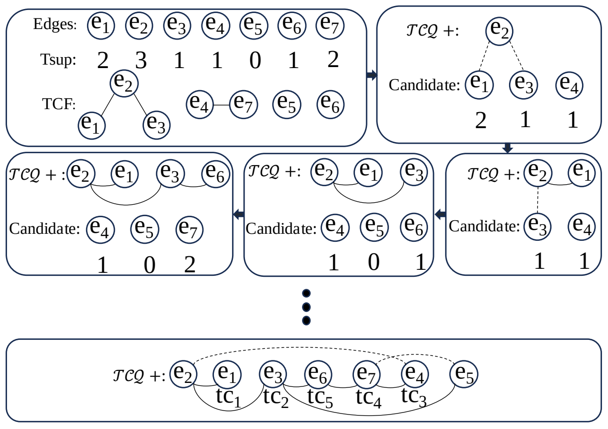

Fig. 7: The construction of $\mathcal{TCQ}+$

the $tsup$ for each query edge is calculated (Lines 9-11). The first edge in $\mathcal{TO}$ is selected as the edge with the highest $tsup$ (Line 13). Subsequent edges within the same forest are selected based on their connection to a neighboring edge in $\mathcal{TO}$ and their $tsup$, with ties broken by choosing the edge with the smallest candidate set (Line 18). This process continues to organize all edges within each forest. When transitioning between forests, the selected edge shares at least one vertex with an edge already in $\mathcal{TO}$ and has the highest $tsup$ (Line 25). For each query edge, its $prec$ and *forward edge* is stored (Lines 20-21 and 27-28). For each *temporal-constraint*, the edge that appears last in $\mathcal{TO}$ is also recorded (Line 30).

Theorem 4 (Complexity of building $\mathcal{TCQ}+$): The time and space complexity of building the $\mathcal{TCQ}+$ graph is $O(|V_q|^2 \cdot d_{\max}^2 + |E_q|^2 + |\mathcal{TC}|)$ and $O(|E_q| + |\mathcal{TC}|))$, respectively.

Proof of THEOREM 4: Initializing the temporal-constraint edge $\mathcal{E}$ and checking cycles (Lines 1-8) takes $O(|V_q|^2 \cdot d_{\max}^2)$, where $d_{\max}$ is the maximum degree of the graph. Computing the support for each query edge (Lines 9-11) takes $O(|E_q| + |\mathcal{TC}|)$. The main loop (Lines 14-29), which involves selecting edges based on support and updating data structures, iterates $O(|E_q|)$ times with each iteration involving $O(|E_q|)$ operations for finding the maximum support and minimum operations, leading to $O(|E_q|^2)$. Therefore, the total time complexity is $O(|V_q|^2 \cdot d_{\max}^2 + |E_q|^2 + |\mathcal{TC}|)$.

Storage for array $tsup$, hash tables $\mathcal{TO}$, $\mathcal{PD}$ and $\mathcal{FE}$ requires $O(|E_q|)$ space. Besides, the hash table $\mathcal{TC}$ require O($|\mathcal{TC}|$). The temporary data structures and variables used during processing also require $O(|E_q|)$ space. Hence, the total space complexity is $O(|E_q| + |\mathcal{TC}|)$.

Example 4: Figure 7 shows the process of constructing $\mathcal{TCQ}+$. The first step involves constructing TCF and calculating the $tsup$ for each edge (recall Figure 2(b)). For instance, given the *temporal-constraint* tc = (2, 3, 5), it is obvious that edge e_2 and e_3 have common vertex u_2, so we build an edge between edge vertices N_{e_2} and N_{e_3}. And also build edges between N_{e_2} and N_{e_1}, between N_{e_4} and N_{e_7}. $tsup[e_1] = 2$; $tsup[e_2] = 3$; ... Then, we choose the edge e_2 with the highest $tsup$, and its neighboring edges (e_1, e_3, e_4) to *candidate*. Next, we choose the neighboring edge e_1 within the same forest that has the highest $tsup$, and build the solid line between e_2 and e_1 (which is stored in $\mathcal{PD}$). Subsequently, we re-compute the neighboring edges of e_2 and e_1, but the candidate are still e_3 and e_4. e_3 is added into the $\mathcal{TCQ}+$, and (e_2, e_3) is added into $\mathcal{PD}$. ... e_4 is added into the $\mathcal{TCQ}+$, and (e_7, e_4) is added into $\mathcal{PD}$ and build the dashed line between e_4 to e_2 (which is stored in $\mathcal{FE}$). This process is iterated for the remaining edges. In the final step, we build the $\mathcal{TC}$ to record the last appears in $\mathcal{TCQ}+$ for both edges in each *temporal constraint*. ($\mathbb{TC}_1 = (2, 1, 3) \rightarrow e_2, e_1 \rightarrow \mathcal{TC}(tc_1) = e_1; \mathbb{TC}_2 = (2, 3, 5) \rightarrow e_2, e_3 \rightarrow \mathcal{TC}(tc_2) = e_3; ...$).

B. Algorithm TCSM-E2E

We also need to generate initial candidates for each query edge. To achieve this, we design a *label degree filter* to determine whether a data edge e_c can match a query edge e, thereby minimizing the size of the candidate set.

Definition 7 (Label Degree Filter(LDF)*):* Given a query graph $G_q = (V_q, E_q, \mathcal{L}_q)$ and a data temporal graph $\mathbb{G} = (\mathcal{V}, \mathcal{E}, \mathcal{L}, \mathcal{T})$. Given $e \in E_q$ and $e_c \in \mathcal{E}$, a *neighbor label filter* (e_c, e) is an injective function h: $e_c \rightarrow e$ that satisfies:

1) $L(e.u) = L(e_c.u)$, $L(e.v) = L(e_c.v)$.
2) $d.in(e_c.u) \geq d.in(e.u)$, $d.out(e_c.u) \geq d.out(e.u)$, $d.in(e_c.v) \geq d.in(e.v)$, $d.out(e_c.v) \geq d.out(e.v)$.

Algorithm 4 presents our TCSM-E2E algorithm, which take $\mathbb{TC}$, G_q and $\mathbb{G}$ as input, and outputs all *TCSM* from G_q to $\mathbb{G}$ under $\mathbb{TC}$. We first find all the possible candidates for each query edge (Lines 1-3). Next, we generate $\mathcal{TO}$, $\mathcal{PD}$, $\mathcal{FE}$, and $\mathcal{TC}$ (Line 4). Then, we start the matching process by expanding the partial match in edge-to-edge manner recursively following $\mathcal{TO}$ (Lines 5-8). If all query edges have been matched, we output the match (Lines 10-11). Otherwise, we obtain the next query edge e in $\mathcal{TO}$, the *prec* of e and set the candidate data edges set of e to empty (Line 13). We extract the candidates data edges of e based on the data edge matched to the *prec* of e and the structural correlation between e and the *prec* of e (Lines 14-16). For each candidate data edge e_c of e, Line 18 checks whether there is an intersection between the candidate data edge and the match of $\mathcal{FE}(e)$. If the query edge e and the already matched query edge can form a temporal constraint (tc), it is necessary to evaluate whether the temporal relationships of the partial match, after incorporating data edge e_c, satisfy the specified tc (Lines 24-26). If so, we expand the partial match by matching the next query edge (Lines 19-20). Otherwise, the algorithm continue to matches the next candidate data edge or backtracks to the last query edge.

Algorithm 4: TCSM-E2E($G_q, \mathbb{TC}, \mathbb{G}$)

```
   input : $G_q$, $\mathbb{TC}$ and $\mathbb{G}$.
   output: all TCSMs $M$ from $G_q$ to $\mathbb{G}$ under $\mathbb{TC}$.
   // generate initial candidate set.
1  for each $e \in E_q$ do
2      for each $e_c \in \mathcal{E}$ do
3          if $LDF(e_c, e)$ is true then $e.C \leftarrow e_c$;
   // generate $\mathcal{TCQ}+$ graph
4  ($\mathcal{TO}$,$\mathcal{PD}$,$\mathcal{FE}$,$\mathcal{TC}$) $\leftarrow$ $\mathcal{TCQ}+$($\mathbb{TC}$, $G_q$, $\mathbb{G}$);
   // matching process.
5  $\lambda \leftarrow 1$, $e \leftarrow \mathcal{TO}[\lambda]$, $M \leftarrow \emptyset$;
6  for each $e_c \in e.C$ do
7      $M[e] \leftarrow e_c$;
8      DFS ($\mathbb{G}$, $\mathcal{TO}$, $\mathcal{PD}$, $\mathcal{FE}$,$\mathcal{TC}$,$M$,$\lambda$+1);
9  Procedure DFS($\mathbb{G}$, $\mathcal{TO}$, $\mathcal{PD}$, $\mathcal{FE}$, $\mathcal{TC}$, $M$, $\lambda$):
10     if $\lambda$ = $|\mathcal{TO}|$ +1 then
11         print $M$;
12     else
13         $e \leftarrow \mathcal{TO}[\lambda]$, $e' \leftarrow \mathcal{PD}[e]$, $e.C \leftarrow \emptyset$;
           // generate candidate in current state
14         for each $e_c \in M[e'].adje$ do
15             if $L(e_c.u)$=$L(e.u)$&$L(e_c.v)$=$L(e.v)$ then
16                 $e.C \leftarrow e_c$;
17         for each $e_c \in e.C$ do
18             if Validate($\mathcal{FE}$, $\mathcal{TC}$,$M$, $e$,$e_c$,$e'$) is true then
19                 $M[e] \leftarrow e_c$;
20                 DFS ($\mathbb{G}$, $\mathcal{TO}$, $\mathcal{PD}$, $\mathcal{FE}$,$\mathcal{TC}$,$M$,$\lambda$+1);
21 Function Validate($\mathcal{FE}$, $\mathcal{TC}$, $M$, $e$, $e_c$, $e'$):
22     if $M[\mathcal{FE}(e)] \cap e_c$ = $\emptyset$ then
23         return false;
24     for each $tc \in \mathbb{TC}$ do
25         if $M$ do not satisfy time constraint $tc$ then
26             return false;
27     return true;
```

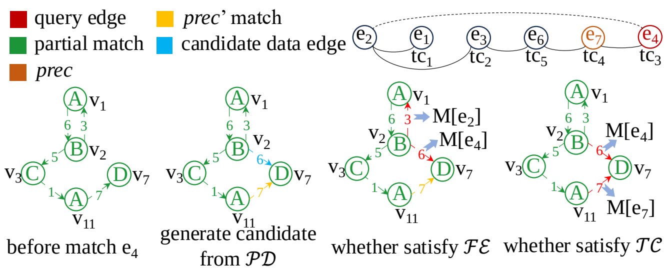

Fig. 8: A specific matching process of algorithm 4.

Example 5: Suppose the current partial match $M = \{e_2{:}(v_2, v_1, 3);\ e_1\ {:}(v_1, v_2, 6);\ e_3{:}\ (v_2, v_3, 5);\ e_6{:}(v_3, v_{11}, 1);\ e_7{:}\ (v_{11}, v_7, 7)\}$, we need to match e_4. The first step involves generating candidate from $\mathcal{PD}$, so we match from the *prec* edge of e_4 from $\mathcal{TCQ}+$. The *prec* edge is e_7 and $M(e_7) = (v_{11}, v_7, 7)$. Among the neighboring edges of $(v_{11}, v_7, 7)$, $\{(v_2, v_7, 6)\}$ is generated, which is an edge between vertex with label same as B and v_7. Then, we check whether the candidate edge satisfy $\mathcal{FE}$. Consider $M(e_4) = (v_2, v_7, 6)$, since $\mathcal{FE}[e_4] = \{e_2\} \rightarrow (v_2, v_7, 6)$ must have common vertex with $M(e_2) = (v_2, v_1, 3)$ in Figure 2(c). There exist a common vertex between $(v_2, v_7, 6)$ and $(v_2, v_1, 3)$, so $M(e_4) = (v_2, v_7, 6)$ can satisfy $\mathcal{FE}$. Next, we check whether the candidate edge satisfy $\mathcal{TC}$. Consider $M(e_4) = (v_2, v_7, 6)$, since $\mathcal{TC}(tc_3) = e_4$, $\mathbb{TC}_3 \rightarrow e_7.t - e_4.t \leq 4$, and $e_7.t = (v_{11}, v_7, 7).t = 7; e_4.t = (v_2, v_7, 6).t = 6$. We can see that $0 \leq 7 - 6 \leq 4$, so $M(e_3) = (v_2, v_7, 6)$ is a correct matching.

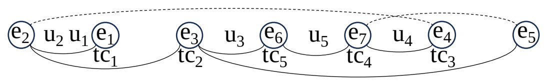

Fig. 9: $\mathcal{TCQ}+$ in algorithm TCSM-EVE.

Theorem 5 (Complexity of Algorithm TCSM-E2E*):* The time and space complexity of Algorithm TCSM-E2E is $O(2^{|E_q|} \times (|E| + d_{\max} + |\mathcal{TC}|))$ and $O(|E_q| + |\mathcal{TC}|)$, respectively.

Proof of THEOREM 5: The initialization (Lines 1-3) involves nested loops over $|E_q|$ and $|E|$ for checking $LDF(e_c, e)$, resulting in $O(|E_q| \times |E|)$. Generating the $\mathcal{TCQ}+$ graph (Line 4) has a time complexity of $O(|E_q|^2 + |V_q| \cdot d^2_{\max} + |\mathcal{TC}|)$. The matching process (Lines 5-20), including DFS and validation, has a worst-case exponential time complexity due to the depth-first search exploring all possible subgraph matchings, leading to $O(2^{|E_q|})$. Each DFS call involves operations that take $O(|E_q| \times |E|)$ and validation steps that add $O(d_{\max})$ per edge check and $O(|TC|)$ per time constraint check. Therefore, the overall time complexity is $O(2^{|E_q|} \times (|E| + d_{\max} + |\mathcal{TC}|))$.

Storage for array $tsup$, hash tables $\mathcal{TO}$, $\mathcal{PD}$ and $\mathcal{FE}$ requires $O(|E_q|)$ space. Besides, the hash table $\mathcal{TC}$ require O($|\mathcal{TC}|$). The candidate set $e.C$ and the mapping M also require $O(|E_q|)$ space. Temporary variables used in loops and recursive calls consume additional $O(|E_q|)$ space. Hence, the total space complexity is $O(|E_q| + |\mathcal{TC}|)$.

C. *Algorithm* TCSM-EVE

The key difference between algorithm TCSM-EVE and algorithm TCSM-E2E lies in whether vertex pre-matching occurs after each edge matching, depending on the addition of a new vertex. Vertex pre-matching helps prune invalid matches by ensuring that when a new query vertex u is added, its matched neighbors align with all *backward neighbors* of u.

Example 6: Figure 9 illustrates the construction of the $\mathbb{TCQ}+$ in the TCSM-EVE algorithm. After each query edge, we check for any newly introduced vertices; if any are present, they are marked accordingly. For instance, when edge e_2 is added, the corresponding vertices u_2 and u_1 are introduced and they are marked after e_2. When edge e_1 is incorporated, no new vertices are introduced and as a result, no vertices are marked. Similarly, when e_3 is added, u_3 is marked after it.

Definition 8 (Backward Neighbor): Given a query graph $G_q = (V_q, E_q, \mathcal{L}_q)$, $\mathcal{PD}$, and a vertex $u \in V_q$ which is added because of query edge e, a *backward neighbor* of u, denoted as $\mathcal{BN}(u)$, is a set that contains all neighbor vertices of u in V_q except the common vertex between e and *prec* of e.

Algorithm 5 outlines our TCSM-EVE algorithm, which shares similarities with the TCSM-E2E; thus, certain portions are omitted for brevity. The matching process begins by recursively expanding the partial match in an edge-to-edge manner according to $\mathcal{TO}$ (Lines 1-3). Before matching the

Algorithm 5: TCSM-EVE$(G_q, \mathbb{TC}, \mathbb{G})$

```
input : $G_q$, $\mathbb{TC}$ and $\mathbb{G}$.
output: all TCSMs $M$ from $G_q$ to $\mathbb{G}$ under $\mathbb{TC}$.
   // generate initial candidate set.
   // ...
   // generate $\mathcal{TCQ}+$ graph
   // ...
   // matching process.
1  $\lambda \leftarrow 1$, $e \leftarrow \mathcal{TO}[\lambda]$, $M \leftarrow \emptyset$;
2  for each $e_c \in e.C$ do
3      $M[e] \leftarrow e_c$;
4      if Vmatch$(e.u, e_c.u)$ & Vmatch$(e.v, e_c.v)$ then
5          DFS($\mathbb{G}$, $\mathcal{TO}$, $\mathcal{PD}$, $\mathcal{FE}$, $\mathcal{TC}$, $M$, $\lambda$+1);
6  Procedure DFS($\mathbb{G}$, $\mathcal{TO}$, $\mathcal{PD}$, $\mathcal{FE}$, $\mathcal{TC}$, $M$, $\lambda$):
7      if $\lambda$ = $|\mathcal{TO}|$ +1 then
8          print $M$;
9      else
10         $e \leftarrow \mathcal{TO}[\lambda]$, $e' \leftarrow \mathcal{PD}[e]$, $e.C \leftarrow \emptyset$;
           // generate candidate in current state
11         for each $e_c \in M[e'].adje$ do
12             if $L(e_c.u)$=$L(e.u)$&$L(e_c.v)$=$L(e.v)$ then
13                 $e.C \leftarrow e_c$;
14         for each $e_c \in e.C$ do
15             if $M[\mathcal{FE}(e)] \cap e_c \neq \emptyset$ & $M \cup e_c$ can satisfy $\mathbb{TC}$ then
16                 $M[e] \leftarrow e_c$;
17                 if $\{e.u, e.v\} - \{e'.u, e'.v\} \neq \emptyset$ then
18                     $u \leftarrow \{e.u, e.v\} - \{e'.u, e'.v\}$;
19                     $v \leftarrow \{e_c.u, e_c.v\} - \{M[e'].u, M[e'].v\}$;
20                     if Vmatch$(u, v)$ then
21                         DFS($\mathbb{G}$, $\mathcal{TO}$, $\mathcal{PD}$, $\mathcal{FE}$, $\mathcal{TC}$, $M$, $\lambda$+1);
22                 else
23                     DFS($\mathbb{G}$, $\mathcal{TO}$, $\mathcal{PD}$, $\mathcal{FE}$, $\mathcal{TC}$, $M$, $\lambda$+1);
24 Function Vmatch($u$, $v$):
25     for each $u' \in BN(u)$ do
26         if $\nexists\ v' \in N(v)$, $L(v')$ = $L(u')$ then
27             return false;
28     return true;
```

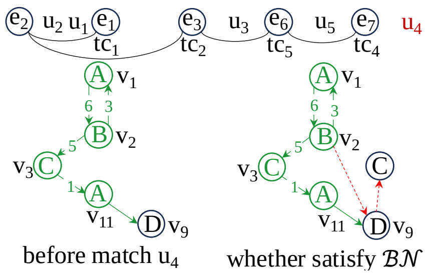

Fig. 10: A specific matching process of algorithm 5.

second query edge, we verify whether the two data vertices of the first edge can match the two query vertices of first query edge. This entails confirming that there are neighboring vertices of the data vertex that can match $\mathcal{BN}(u)$ of query vertex u. If so, we proceed to match the next edge (Lines 4-5). Upon matching all query edges, we output the match (Lines 7-8). If not, we retrieve the next query edge e, generating the candidate data edges set for e (Lines 10-13). For each candidate data edge e_c of e, Line 15 evaluates the structural and temporal constraints of the match between the candidate edge and the query edge. If a match is feasible, we include it in the partial match (Line 16), and we check whether a new vertex emerges in this layer of edge matching (Line 17). If no not, we proceed to match the next query edge (Line 23). However, if a new vertex does emerge, we assess whether this data vertex can match the corresponding query vertex (Line 20). If the newly added vertex can be matched, we continue matching the next query edge (Lines 23).

Example 7: To facilitate a better understanding of Algorithm 5 better, we provide the following illustrative example. When matching newly added vertex u_4 after edge e_7 is matched, we find that $\mathcal{BN}(u_4) = \{u_2, u_3\}$. We need to check whether the neighbor vertex of v_9 (the match of u_4) can match both u_2 and u_3. For simplicity, we will assume that a match is feasible if the labels correspond. The label of u_2 and u_3 is B and C, respectively. In Figure 2(c), v_9 has neighboring vertices with labels B and A, allowing it to match u_2, but not u_3.

Theorem 6 (Complexity of Algorithm TCSM-EVE*):* The time and space complexity of Algorithm TCSM-EVE is $O(2^{|E_q|} \times (|E| + d_{\max} + |TC|))$ and $O(|E_q| + |\mathcal{TC}|)$, respectively.

Proof of THEOREM 6: The initialization and generating of the $\mathcal{TCQ}+$ graph (omitted details) involve operations similar to those in previous algorithms, which typically take $O(|E_q|^2 + |V_q|^2 \cdot d_{\max}^2 + |TC|)$. The matching process (Lines 1-6) involves nested loops over the candidate set $e.C$ and checking vertex matches, leading to $O(|E_q| \times |E|)$. The DFS procedure (Lines 7-25) explores all possible subgraph matchings, resulting in a worst-case exponential complexity of $O(2^{|E_q|})$. Each DFS call and the function $Vmatch$ (Lines 26-30) involve operations that add $O(d_{\max})$ per edge check and $O(|TC|)$ per time constraint check, thus the overall time complexity is $O(2^{|E_q|} \times (|E| + d_{\max} + |TC|))$.

Storage for array $tsup$, hash tables $\mathcal{TO}$, $\mathcal{PD}$ and $\mathcal{FE}$ requires $O(|E_q|)$ space. Besides, the hash table $\mathcal{TC}$ require O($|\mathcal{TC}|$). The candidate set $e.C$ and the mapping M also require $O(|E_q|)$ space. Temporary variables used in loops and recursive calls consume additional $O(|E_q|)$ space. Hence, the total space complexity is $O(|E_q| + |\mathcal{TC}|)$.

Example 8: Figure 11 illustrates the matching trees generated by our algorithms. As shown, edge-based matching outperforms vertex-based matching by reducing the size of the matching tree and significantly enhancing efficiency. Additionally, integrating vertex matching further minimizes the tree size by pruning unsuitable matches early in the process. Thus, the TCSM-EVE algorithm achieves superior pruning effectiveness compared to the other two algorithms, as further confirmed in subsequent experiments. Figure 11(a) presents the matching process obtained using the TCSM-V2V algorithm, as applied to Figure 2. The match $M = \{u_2 : v_2; u_1 : v_1; u_4 : v_7; u_5 : v_{11}; u_3 : v_3\}$ is identified as a valid match (highlighted within a dotted box). The remaining matches either fail to structurally align with the query graph, do not satisfy the temporal constraints, or are unable to generate the corresponding candidate vertices. For instance, consider the match $M = \{u_2 : v_2; u_1 : v_1; u_4 : v_7; u_5 : v_{11}; u_3 : v_4\}$, which does not structurally match the query graph. In this

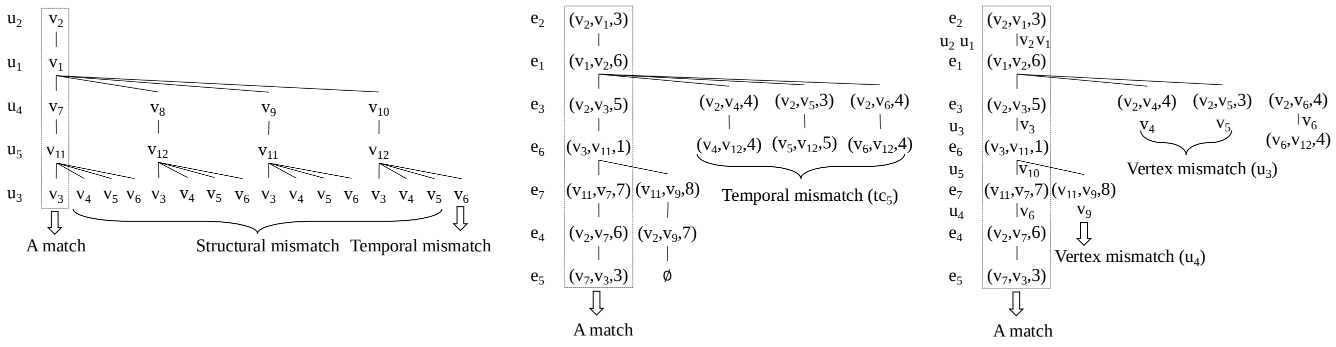

(a) Algorithm **TCSM-V2V** (b) Algorithm **TCSM-E2E** (c) Algorithm **TCSM-EVE**

Fig. 11: The matching trees of our algorithms.

case, there should be edges between v_4 and v_{11}, as well as between v_4 and v_7 (corresponding to edges between u_3 and u_5 and between u_3 and u_4 in the query graph), but such edges are absent. Conversely, the match $M = \{(u_2 : v_2; u_1 : v_1; u_4 : v_{10}; u_5 : v_{12}; u_3 : v_6\}$ fails to satisfy the temporal constraints. Constraint tc_5 indicates that the edge between v_6 and v_{12} must correspond to the edge between v_2 and v_1 in terms of timing, with a time difference of less than 3 ($0 \leq e_2.t - e_6.t \leq 3 \rightarrow 0 \leq (M[u_2], M[u_1]).t - (M[u_3], M[u_5]).t \leq 3 \rightarrow 0 \leq (v_2, v_1).t - (v_6, v_{12}).t \leq 3 \rightarrow 0 \leq 3 - 4 \leq 3$). Figure 11(b) presents the matching process obtained using the TCSM-E2E algorithm, as applied to Figure 2. The match M = $\{e_2$:$(v_2, v_1, 3)$; e_1 :$(v_1, v_2, 6)$; e_3: $(v_2, v_3, 5)$; e_6:$(v_3, v_{11}, 1)$; e_7: $(v_{11}, v_7, 7)$; e_4: $(v_2, v_7, 6)$; e_5:$(v_7, v_3, 3)\}$ is identified as a valid match (highlighted within a dotted box). The remaining matches either fail to structurally align with the query graph, do not satisfy the temporal constraints, or are unable to generate the corresponding candidate data edges. For example, the match $M = \{e_2$:$(v_2, v_1, 3)$; e_1 :$(v_1, v_2, 6)$; e_3: $(v_2, v_4, 4)$; e_6:$(v_4, v_{12}, 4)\}$ fails to satisfy the temporal constraints. Constraint tc_5 indicates that the time associated with the edge $(v_4, v_{12}, 4)$ must be less than that of the edge $(v_2, v_1, 3)$, with a difference of less than 3 ($0 \leq e_2.t - e_6.t \leq 3 \rightarrow 0 \leq (v_2, v_1, 3).t - (v_4, v_{12}, 4).t \leq 3 \rightarrow 0 \leq 3 - 4 \leq 3$). However, the matches for e_6 and e_2 clearly do not conform to this temporal relationship. In another partial match, $M = \{e_2$:$(v_2, v_1, 3)$; e_1 :$(v_1, v_2, 6)$; e_3: $(v_2, v_3, 5)$; e_6:$(v_3, v_{11}, 1)$; e_7: $(v_{11}, v_9, 8)$; e_4: $(v_2, v_9, 7)\}$, when attempting to match e_5, the match of e_5's *prec* $(v_2, v_3, 5)$ fails to find a neighboring edge directed toward v_3 from a vertex labeled D. As a result, there are no corresponding candidate edges. Figure 11(c) show the matching process of using TCSM-EVE algorithm. The match $M = \{((v_3, v_1, 3)$, $e_2)$, (v_3, u_2), (v_1, u_1), $((v_1, v_3, 6)$, $e_1)$, $((v_3, v_{14}, 5)$, $e_3)$, (v_{14}, u_3), ($(v_{14}, v_{18}, 1)$, $e_6)$, (v_{18}, u_5), $((v_{18}, v_7, 7)$, $e_7)$, (v_7, u_4), $((v_3, v_7, 6)$, $e_4)$, $((v_7, v_{14}, 3)$, $e_5))\}$ is a correct match. Such as the candidate data vertex v_4 to match u_3, the partial match $M = \{(v_2, v_1, 3)$: e_2; u_2, v_2 :; u_1 : v_1; e_1: $(v_1, v_2, 6)$; e_3:$(v_2, v_4, 4)\}$. u_3 have *backford neighbor* u_4 and u_5 with label D, A, respectively. But, the data vertex v_4 only have two neighbors vertex with B, A. So, the data vertex v_4 can not match u_3.

TABLE II: Data Temporal Graph $\mathbb{G}$

Dataset	$\lvert V\rvert$	$\lvert\mathcal{E}\rvert$	$\lvert E\rvert$	Time span	avgd
CM	1,899	59,835	20,296	193 days	31.5
EE	986	332,334	24,929	803 days	337
MO	24,818	506,550	239,978	2,350 days	20.41
UB	159,316	964,437	596,933	2,613 days	6.05
SU	194,085	1,443,339	924,886	2,773 days	7.43
WT	1,140,149	7,833,140	3,309,592	2,320 days	6.87

V. EXPERIMENTS

A. *Experimental setup*

In this section, we evaluate the performance of the algorithms we proposed across various datasets and query configurations. We implement all our algorithms in C++. All experiments are conducted on a Linux machine equipped with a 2.9GHz AMD Ryzen 3990X CPU and 256GB RAM running CentOS 7.9.2 (64-bit). The experimental results are meticulously detailed in the subsequent parts of this section.

Datasets. We utilize 7 datasets that have been commonly used for evaluating previous temporal subgraph matching methods [28]. Table II presents their statistics. All the datasets are downloaded from https://snap.stanford.edu/data/ and are listed in increasing order of the number of edges. CM (*CollegeMsg*) is the datasets of messages on a facebook-like platform at UC-Irvine. EE (*email-Eu-core-temporak*) is the datasets of e-mails between users at a research institution. MO (*sx-mathoverflow*) is the datasets of comments, questions, and answers on Math Overflow. UB (*sx-askubuntu*) is the datasets of comments, questions, and answers on Ask Ubuntu. SU (*sx-superuser*) is the datasets of comments, questions, and answers on Super User. WT (*wiki-talk-temporal*) is the sets of users editing talk pages on Wikipedia.

Queries and Temporal-Constriants. We employed three labeled queries and three temporal constraints between edges, as illustrated in Figure 12. Each of these three queries comprises six nodes, while the temporal constraints vary in structure, being linear, tree-shaped, and graph-shaped, respectively. Furthermore, we conducted experiments with queries

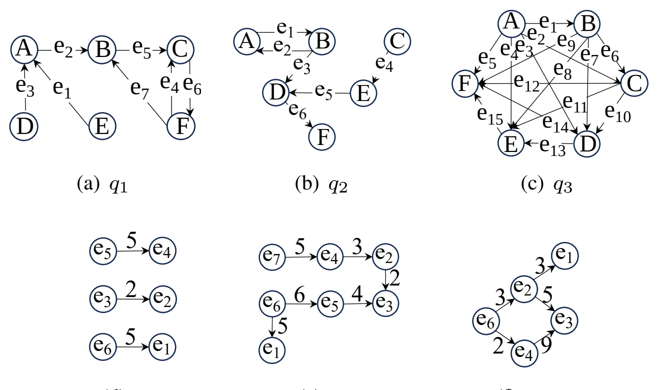
(a) q_1 (b) q_2 (c) q_3

(d) tc_1 (e) tc_2 (f) tc_3

Fig. 12: Queries q and Temporal-Constriants tc.

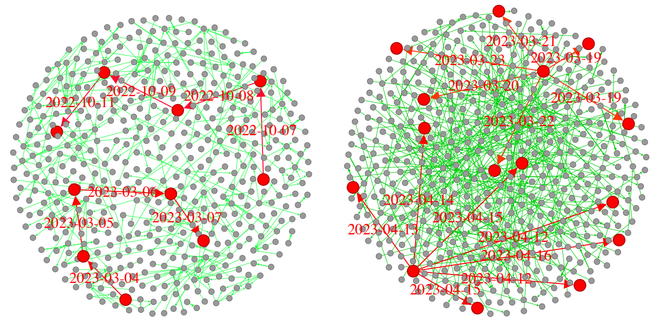
(a) rapid fund circulation pattern (b) online brushing pattern

Fig. 13: Common fraudulent detection in Ant Group.

containing more vertices and temporal constraints featuring more edges, yielding similar conclusions. However, due to space limitations, we refrain from reporting on those cases here. Additionally, unless otherwise specified, comparisons are made between query graph q_1 and *temporal-constraint* tc_2.

Algorithms. We established a baseline using a static subgraph matching algorithm RI-DS [26], with an additional *temporal constraint*. For comparison, we included several continuous subgraph matching algorithms, SymBi [14], Turboflux [15], Graphflow [29], SJ-Tree [30], and IEDyn [31]. Additionally, RapidFlow [10], CaLiG [12], NewSP [11] are the sota algorithms in continuous subgraph matching, so we also modified algorithms to satisfy *temporal-constriants* as our baseline.

B. Case Study

As illustrated in Figure 13, the application of our method in the detection of fradulent at Ant Group provides a concrete example. In telecom fraud, the flow of funds typically exhibits the characteristic of rapid circulation. Therefore, we can employ a linear graph structure, where each subsequent edge has a larger timestamp than the previous one, with a minimal time difference, to detect such fraudulent activities. And user behaviors associated with online brushing often manifest as transactions with different merchants and temporal intervals between each transaction. Thus, we can utilize a star-shaped graph structure, where adjacent edges have distinct time differences, to identify such activities. In practical applications, however, not all matched results correspond to fraudulent users. Additional information is required to ultimately determine whether the matched users are indeed engaging in fraudulent activities. In the actual implementation at Ant Group, our method achieved an accuracy rate of over 50%, which is significantly superior to other detection approaches.

TABLE III: Running time of various methods (second).

Methods	CM	EE	MO	UB	SU	WT
Symbi	0.004	0.003	0.197	0.199	0.289	4.377
Turboflux	0.004	0.033	0.174	0.267	0.357	6.118
Graphflow	0.001	0.183	0.128	0.108	0.146	5.164
SJ−Tree	0.023	0.030	0.319	0.180	0.231	56.67
IEDyn	0.003	0.003	0.185	0.195	0.323	4.981
RapidFlow	0.379	1.905	2.502	5.939	8.898	44.30
CaLiG	0.305	1.847	26.99	422.7	84.15	17682
NewSP	0.240	1.886	10.16	22.46	15.76	368.9
RI−DS	0.132	0.103	13.88	47.058	44.668	4071
TCSM−V2V	0.001	0.011	0.120	0.138	0.168	3.941
TCSM−E2E	0.008	0.102	0.118	0.089	0.125	3.518
TCSM−EVE	0.008	0.091	0.114	0.089	0.114	2.475

C. Experimental Results

Exp-1: Running time of various methods. Table V delineates a comparative evaluation of the performance metrics of five static subgraph matching algorithms and four modified temporal algorithms, juxtaposed with our proposed methodologies across six distinct datasets. The empirical findings reveal that our algorithms exhibit performance on par with extant methods on smaller datasets, such as EE. However, they manifest enhanced efficiency on medium-sized datasets when contrasted with conventional matching algorithms. Notably, on large-scale datasets encompassing millions of vertices, our algorithms markedly surpass existing methodologies, thereby highlighting their unparalleled efficiency and scalability. While these static algorithms may ostensibly exhibit satisfactory performance, they fundamentally eschew the integration of *temporal-constraints* within their computational paradigms. Theoretical postulations suggest that the assimilation of *temporal-constraints* into the computational process is likely to precipitate a diminution in performance. In light of these considerations, our algorithm evinces a pronounced superiority in efficacy relative to these static approaches.

Exp-2: The runtime distribution for building $\mathcal{TCQ}$(+) and performing matching. Figure 14 illustrates bar chart depicting the runtime distribution for building $\mathcal{TCQ}$(+) and performing matching across the MO, UB and SU.The construction of $\mathcal{TCQ}$(+) by algorithms TCSM-E2E and TCSM-EVE takes more time than algorithm TCSM-V2V, with algorithm TCSM-EVE requiring slightly more time than algorithm TCSM-E2E. Conversely, the execution of the matching process shows the opposite trend. This indicates that the efficiency of algorithms TCSM-E2E and TCSM-EVE primarily attributed to the effectiveness of their $\mathcal{TCQ}$ construction.

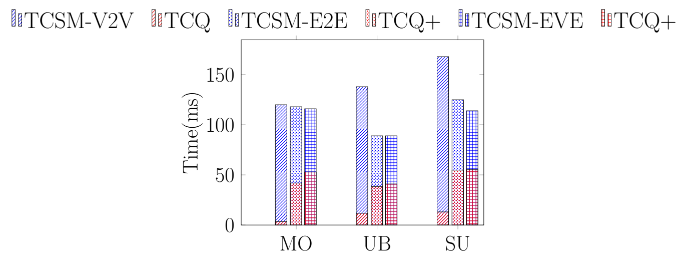

Fig. 14: Runtime distribution.

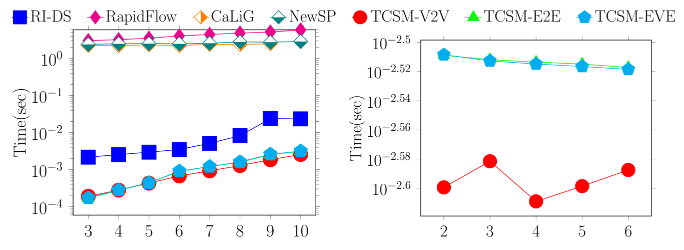

(a) vary $|q|$ on UB (b) vary $|tc|$ on UB

Fig. 15: Runtime with different $|q|$ or $|tc|$.

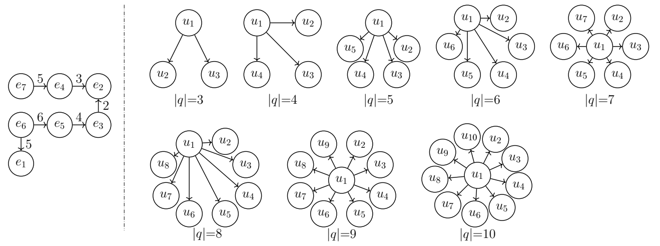

(a) exp-3 (a)

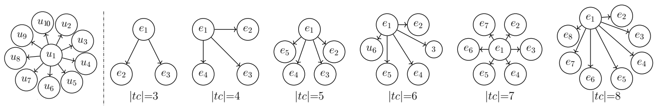

(b) exp-3 (b)

Fig. 16: The query graph and temporal-constraints of exp-3.

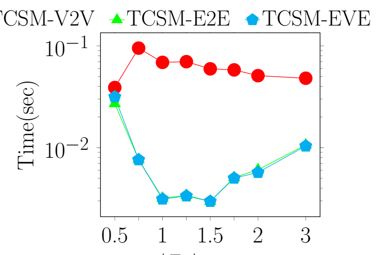

(a) vary $\frac{|E_q|}{|V_q|}$ on UB

Fig. 17: Runtime with queries of different density.

Exp-3: Scalability with different size of queries and *temporal-constraints*. Figure 15 presents line charts showing the running times of various algorithms across a series of queries, with $|q|$ ranging from 3 to 10 and $|tc|$ varying from 2 to 6 on UB. The results reveal that running times generally increase for all algorithms as $|q|$ grows, reflecting the corresponding rise in computational complexity. Since these baseline algorithms are not designed for temporal graphs, changes in $|tc|$ do not influence their performance, and thus they are excluded. The runtime of the TCSM-V2V algorithm initially increases, then decreases sharply, and finally experiences a gradual rise as $|tc|$ grows. In contrast, the TCSM-E2E and TCSM-EVE algorithms demonstrate a trend of gradually decreasing runtime as $|tc|$ increases. These observations indicate that the TCSM-E2E and TCSM-EVE algorithms offer better stability compared to TCSM-V2V.

Exp-4: Scalability with query graph of different density. Figure 17 illustrates line charts depicting the running times of various algorithms across the UB, with density ranging from 0.5 to 3. Notably, the TCSM-E2E and TCSM-EVE algorithms demonstrated optimal performance when the density near 1 to 1.5, suggesting that a balanced density of query graph enhances their efficiency by simplifying graph topology. In contrast, the TCSM-V2V algorithm exhibited diminished performance when the density of query approached 1, indicating that it may depend on a more complex graph structure for optimal operation, likely due to its specific methodology for handling vertex-to-vertex comparisons.

Exp-5: Scalability with different data temporal graphs. We conducted experiments to assess the scalability of our algorithms by varying $|\mathcal{E}|$ in the original graph, generating four subgraphs for each dataset, and comparing the running times of all algorithms on these subgraphs. The results for the large graphs UB and SU dataset are shown in Figure 18. As $|\mathcal{E}|$ changes, the runtimes of TCSM-V2V, TCSM-E2E and TCSM-EVE increase smoothly. Moreover, across all parameter settings, our algorithm are significantly faster than these baseline algorithms, reaffirming the findings from Exp-2 again.

Exp-6: Memory usages. Table IV compares memory usage across all algorithms on multiple datasets. For smaller datasets, our proposed algorithms use less memory, whereas on larger datasets, their memory usage exceeds that of the baseline algorithms but stays within an acceptable range. The memory usage of the TCSM-E2E and TCSM-EVE algorithms is similar and slightly higher than that of the TCSM-V2V algorithm.

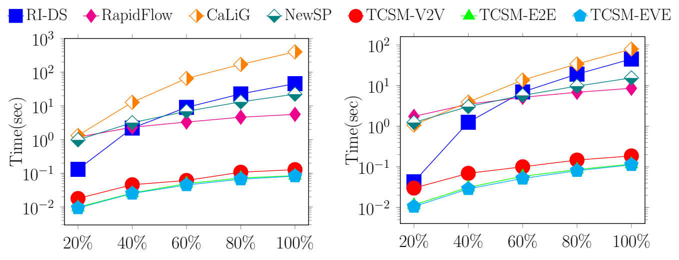

(a) vary $|\mathcal{E}|$ on UB (b) vary $|\mathcal{E}|$ on SU

Fig. 18: Runtime with different data temporal graph.

TABLE IV: The memory usages of the algorithms (MB).

Methods	CM	EE	MO	UB	SU	WT
Symbi	143	143	158	236	241	339
Turboflux	143	143	158	233	237	333
Graphflow	143	143	148	188	188	234
SJ−Tree	143	143	148	188	188	7977
IEDyn	143	143	155	222	225	308
RI−DS	114	115	121	145	121	165
RapidFlow	4.4	10.8	31	118	139	295
CaLiG	4.5	10.8	24	121	135	212
NewSP	4.4	10.9	28.4	101	117	163
TCSM−V2V	3.6	4.2	16.9	80	88.5	88.9
TCSM−E2E	5.1	11.7	34.6	143	158	512
TCSM−EvE	5.3	85.2	34.6	166	184	608

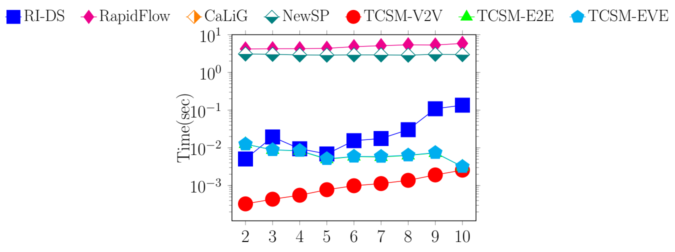

Fig. 19: Runtime with vary $|\mathcal{L}_q|$ on UB.

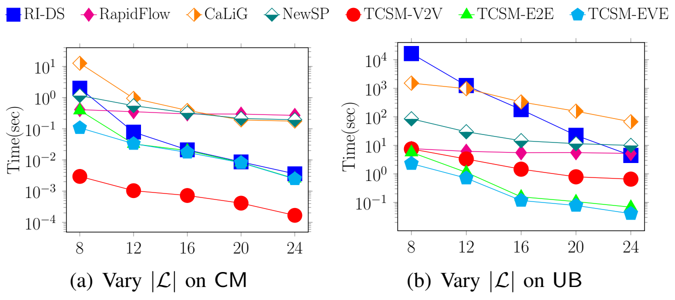

(a) Vary $|\mathcal{L}|$ on CM (b) Vary $|\mathcal{L}|$ on UB

Fig. 20: Runtime with $\mathbb{G}$ of different number of labels.

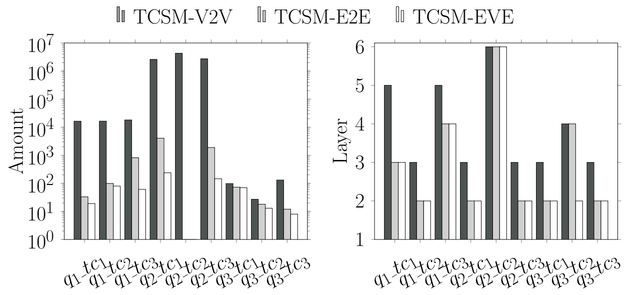

Fig. 21: Observations on failed enumeration in the UB.

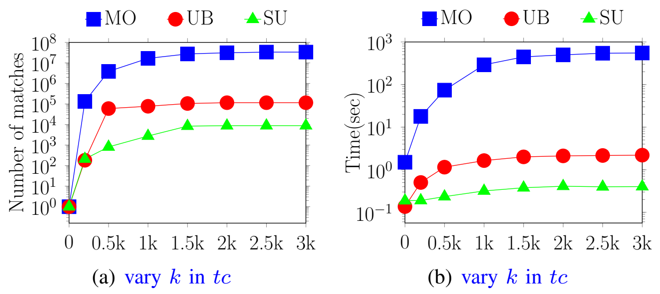

(a) vary k in tc (b) vary k in tc

Fig. 22: Number of matches and runtime with vary k.

Exp-7: The effect of queries q with vary $|\mathcal{L}_q|$. Figure 19 illustrates the runtime performance of all algorithms when querying a dataset with varying $|\mathcal{L}_q|$. As $|\mathcal{L}_q|$ increases, the baseline algorithms and TCSM-V2V algorithms exhibit a general upward trend in runtime, while the TCSM-E2E and TCSM-EVE algorithms display a decreasing trend with relatively minor performance differences between them. Notably, RI-DS reaches a local maximum in runtime when $|\mathcal{L}_q|$ is three.

Exp-8: The effect of data temporal graph $\mathbb{G}$ with vary $|\mathcal{L}|$. We generated five data graphs, each with a distinct $|\mathcal{L}|$: 8, 12, 16, 20, and 24. Figure 20 illustrates the performance of all algorithms on these synthetic datasets as $|\mathcal{L}|$ increases. The runtime of all algorithms exhibits a declining trend as $|\mathcal{L}|$ grows. Our algorithms consistently outperform all baseline algorithms, likely due to their more sophisticated handling of labels and graph structures. For smaller datasets, TCSM-V2V demonstrates the best performance, indicating that its vertex-focused approach is particularly effective when dealing with fewer data vertices. Conversely, for larger datasets, TCSM-E2E and TCSM-EVE prove to be more efficient, as they better manage increased connectivity and complex edge data graph.

Exp-9: Observations on Failed Enumeration. We designed experiments to observe the total occurrences of failed enumerations and the specific layer in the matching tree where the first failed enumeration occurred, which can serve as an indicator of pruning efficiency. Figure 21 compares the occurrences of failed enumeration and the layer of first failed enumeration across all algorithms on UB. The results indicate that the number of failed enumerations in edge-based matching is lower than that in vertex-based matching, and the first failed enumeration occurs at a shallower layer in the matching tree. Additionally, the TCSM-EVE algorithm exhibits slightly fewer failed enumerations compared to TCSM-E2E, reflecting a higher level of algorithmic efficiency.

Exp-10: Number of matches and runtime with vary interaction time gaps k. Figure 22 illustrates line charts depicting the number of matched instances and running times of various interaction time gaps k in tc across the MO, UB and SU datasets, with k ranging from 0 to 3000. Based on the experimental results, it is evident that as the interaction time gap k increases, the number of matched instances exhibits a rapid growth followed by stabilization, with the computational runtime demonstrating a similar pattern. This phenomenon aligns with real-world observations, where a larger interaction time window inherently includes more potential matches, albeit at the cost of incorporating less relevant instances. An excessively large time gap may lead to increased false positives by misclassifying legitimate transactions as fraudulent. Therefore, the optimal configuration of the interaction time gap is crucial for achieving accurate identification of relevant fraudulent transactions while maintaining system precision.

VI. Related Work

A. Subgraph isomorphism on static graphs

Filtering-Based Methods. Several filtering methods focus on features. For instance, label-and-degree filtering [33], [35] considers a data vertex v a candidate for query vertex u if v shares the same label as u and has a degree at least as high as u. Neighborhood label frequency filtering [27] checks if a candidate has sufficient neighbors with matching labels compared to u. Recent approaches combine these methods and incorporate pseudo-matching on nearby vertices or utilize a spanning tree or *DAG* from the query graph [7], [36]–[38].

Ordering-Based Methods. The size of the search space depends heavily on the order in which the query vertices are matched. This is because the target of the query vertex u must be selected from data vertices that are adjacent to the targets of all previously matched neighbors of u. Several efforts have been made to generate an optimal matching order by first determining the target for the query vertex with the fewest candidate vertices, thus keeping the search space for the remaining query vertices small [1], [6], [38]–[40]. However, there is no universal method for generating an optimal ordering for arbitrary query graphs and data graphs [2], [41]. Therefore, it is crucial to minimize the number of candidates.

Enumeration-Based Methods. These algorithms typically adopt a recursive enumeration procedure to find all matches and can be categorized into three types. The first, known as Direct Enumeration, directly explores the data graph to find all results, exemplified by *QuickSI* [43], *RI* [26], and *VF2++* [44]. The second type, Indexing Enumeration, constructs indexes on the data graph and uses these indices to answer queries, as seen in *GADDI* [45], *SUFF* [46], *HUGE* [47], *Circinus* [48] and *SGMatch* [49]. The third type, Preprocessing Enumeration, generates candidate vertex sets for each query at runtime and evaluates the query based on these sets. This method is widely used in recent database community algorithms, such as *GraphQL* [50], *TurboISO* [51], and *CECI* [7].

B. Subgraph isomorphism on temporal graphs

While subgraph isomorphism in static graphs is well-studied, the temporal variant has received less attention, with only a few algorithms addressing the Temporal Subgraph Isomorphism (TSI) problem [1], [13], [22], [52]–[57]. For instance, [53] sorts edges by their time series before matching, while others [13], [22], [52], [54] focus on edge-by-edge matching under global time constraints. Earlier research [58] employed a vertex-by-vertex approach similar to the RI algorithm [26]. Additional studies explore temporal graph pattern matching using database query techniques [59]–[61]. Related to TSI is the identification of temporal motifs, which are small, recurrent subgraphs characterized by k vertices or m edges [62], [63]. The definition of a temporal motif, as introduced in [10], [64], involves matching a small query pattern with edges that follow a specific order, although these studies mainly focus on counting motifs of 2 or 3 edges. Other refinements include constraining timestamp offsets [65] and finding motifs with flow constraints [66]. [20], [24], [25] define edge order and global time window, which can address some $TCSM$ problems where edges have sequential relationships but do not emphasize temporal intervals between edges.

VII. Conclusion

We address the problem of Temporal-Constraint Subgraph Matching (*TCSM*), which is inherently *NP-hard*. Traditional techniques, such as candidate filtering, often struggle with the complexities of $TCSM$. To overcome these challenges, we developed three novel algorithms: TCSM-V2V, which utilizes vertex-to-vertex expansion and leverages temporal constraints to minimize duplicate matches; TCSM-E2E, which applies edge-to-edge expansion, significantly reducing matching time by minimizing vertex permutations; and TCSM-EVE, which adopts an interactive edge-vertex-edge expansion strategy, eliminating both vertex and edge permutations to further reduce duplicate matches. Extensive experiments on seven real-world temporal datasets which popularly used demonstrate that our algorithms consistently outperform existing methods, achieving substantial reductions in matching time.

TABLE V: Running time of various q and tc (second).

DataSet	q, tc	RapidFlow	CaLiG	NewSP	RI−DS	TCSM−V2V	TCSM−E2E	TCSM−EVE
CM	q_1, tc_1	0.3066	0.2797	0.2568	0.0132	0.0003	0.0068	0.0019
	q_1, tc_2	0.3794	0.3049	0.2868	0.0132	0.0003	0.0079	0.0020
	q_1, tc_3	0.2916	0.2596	0.2737	0.0132	0.0002	0.0087	0.0046
	q_2, tc_1	0.2327	0.3304	0.2823	0.0155	0.0002	0.0034	0.0009
	q_2, tc_2	0.2568	0.4987	0.2443	0.0152	0.0002	0.0040	0.0009
	q_2, tc_3	0.2665	0.3389	0.2338	0.0152	0.0004	0.0410	0.0070
	q_3, tc_1	0.3197	0.2449	0.4496	0.0011	0.0002	0.0240	0.0045
	q_3, tc_2	0.3284	0.2371	0.4207	0.0006	0.0003	0.0205	0.0044
	q_3, tc_3	0.3244	0.2376	0.4158	0.0011	0.0002	0.0202	0.0048
EE	q_1, tc_1	1.7455	1.8149	1.8400	0.0630	0.0092	0.1181	0.0241
	q_1, tc_2	1.9047	1.8466	1.9549	0.0643	0.0082	0.0987	0.0217
	q_1, tc_3	1.7661	1.9331	1.9384	0.0640	0.0013	0.0731	0.0406
	q_2, tc_1	1.6057	2.9238	1.7520	0.0327	0.0021	1.0773	0.943
	q_2, tc_2	1.6136	4.0460	1.7510	0.0331	0.0018	0.1556	0.0401
	q_2, tc_3	1.6647	3.0905	1.7341	0.0331	0.0029	0.0890	0.0746
	q_3, tc_1	2.4665	1.4846	10.926	0.0041	0.0011	0.3780	0.0919
	q_3, tc_2	2.4958	1.5530	10.908	0.0040	0.0008	0.3750	0.0911
	q_3, tc_3	2.5434	1.5217	10.908	0.0041	0.0009	0.3760	0.0925
MO	q_1, tc_1	2.3594	35.124	11.112	14.328	0.2813	0.1792	0.1557
	q_1, tc_2	2.5016	26.988	10.375	13.883	0.1197	0.1179	0.1140
	q_1, tc_3	2.3838	25.334	10.252	14.318	0.0665	0.0588	0.0578
	q_2, tc_1	2.1864	38.059	3.4948	2.5363	0.0582	0.0571	0.0187
	q_2, tc_2	2.1393	62.149	3.8069	2.4564	0.0460	0.0407	0.0124
	q_2, tc_3	2.2199	39.22	3.5796	2.5365	0.0709	0.0467	0.0150
	q_3, tc_1	3.3964	21.604	172.93	0.1299	0.1067	0.0801	0.0750
	q_3, tc_2	3.3881	21.837	173.23	0.1280	0.0445	0.0706	0.0526
	q_3, tc_3	3.3729	21.2	172.04	0.1249	0.0630	0.0944	0.0626
UB	q_1, tc_1	5.4634	133.97	21.08	46.095	0.1832	0.0478	0.0440
	q_1, tc_2	5.4821	422.67	22.463	47.058	0.1382	0.0891	0.0878
	q_1, tc_3	5.587	379.02	21.773	46.283	0.1154	0.0679	0.0558
	q_2, tc_1	5.1618	162.27	8.3841	20.412	0.1773	0.0691	0.0464
	q_2, tc_2	5.3085	313.83	9.099	21.141	0.1492	0.0378	0.0287
	q_2, tc_3	5.2299	211.16	8.5278	20.948	0.1925	0.0739	0.0474
	q_3, tc_1	8.4811	207.65	1556.2	0.2900	0.1723	0.1407	0.1330
	q_3, tc_2	8.6135	208.54	1558.5	0.2943	0.1449	0.1717	0.1200
	q_3, tc_3	8.4854	207.79	1555.4	0.2914	0.1324	0.1248	0.1186
SU	q_1, tc_1	8.3922	90.407	16.161	43.368	0.2674	0.0775	0.0636
	q_1, tc_2	8.8983	84.146	15.757	44.668	0.1683	0.1248	0.1136
	q_1, tc_3	8.6361	76.991	15.526	44.579	0.1507	0.0689	0.0664
	q_2, tc_1	8.0775	571.22	15.451	77.757	0.1925	0.1537	0.1422
	q_2, tc_2	8.0541	1466.1	16.238	77.761	0.2723	0.0705	0.0508
	q_2, tc_3	8.189	876.35	15.424	77.878	0.2184	0.1518	0.0681
	q_3, tc_1	11.033	133.13	1374.6	7.0245	0.1325	0.0912	0.0640
	q_3, tc_2	10.642	132.5	1378.3	7.0433	0.1237	0.0680	0.0602
	q_3, tc_3	10.774	131.49	1373.6	7.0387	0.1050	0.0635	0.0625

TABLE VI: The runtime distribution for building TCQ (or others microbenchmarks) and performing matching (ms).

Methods	MO		UB		SU	
	processing	matching	processing	matching	processing	matching
Symbi	24.19	70.41	199.9	21.33	207.2	57.75
Turboflux	42.66	32.03	190.0	79.01	238.5	158.0
Graphflow	0.037	32.16	0.037	32.99	0.037	37.03
SJ−Tree	6.260	364.7	34.00	51.78	36.77	197.3
IEDyn	31.66	153.0	151.2	49.53	136.0	139.4
RI−DS	0.003	13882	0.003	47058	0.004	44668
TCSM−V2V	3.434	116.6	11.75	126.3	13.10	154.9
TCSM−E2E	41.89	76.12	38.28	50.72	54.79	70.21
TCSM−EvE	52.94	61.06	40.99	48.01	55.19	58.81

References

[1] S. Sun and Q. Luo, "Subgraph matching with effective matching order and indexing," *IEEE Trans. Knowl. Data Eng.*, vol. 34, no. 1, pp. 491–505, 2022.

[2] S. Shixuan and L. Qiong, "In-memory subgraph matching: An in-depth study," in *SIGMOD*, 2020, pp. 1083–1098.

[3] J. Arai, Y. Fujiwara, and M. Onizuka, "Gup: Fast subgraph matching by guard-based pruning," *Proc. ACM Manag. Data*, vol. 1, no. 2, pp. 167:1–167:26, 2023.

[4] T. Jin, B. Li, Y. Li, Q. Zhou, Q. Ma, Y. Zhao, H. Chen, and J. Cheng, "Circinus: Fast redundancy-reduced subgraph matching," *Proc. ACM Manag. Data*, vol. 1, no. 1, pp. 12:1–12:26, 2023.

[5] Z. Zhang, Y. Lu, W. Zheng, and X. Lin, "A comprehensive survey and experimental study of subgraph matching: Trends, unbiasedness, and interaction," *Proc. ACM Manag. Data*, vol. 2, no. 1, pp. 60:1–60:29,

2024.
[6] V. Bonnici and R. Giugno, "On the variable ordering in subgraph isomorphism algorithms," *IEEE ACM Trans. Comput. Biol. Bioinform.*, vol. 14, no. 1, pp. 193–203, 2017.
[7] B. Bhattarai, H. Liu, and H. H. Huang, "CECI: compact embedding cluster index for scalable subgraph matching," in *SIGMOD*, 2019, pp. 1447–1462.
[8] W. Shin, S. Song, K. Park, and W. Han, "Cardinality estimation of subgraph matching: A filtering-sampling approach," *VLDB*, vol. 17, no. 7, pp. 1697–1709, 2024.
[9] Z. Jiang, S. Zhang, X. Hou, M. Yuan, and H. You, "IVE: accelerating enumeration-based subgraph matching via exploring isolated vertices," in *IEEE*. IEEE, 2024, pp. 4208–4221.
[10] S. Sun, X. Sun, B. He, and Q. Luo, "Rapidflow: An efficient approach to continuous subgraph matching," *Proc. VLDB Endow.*, vol. 15, no. 11, pp. 2415–2427, 2022.
[11] Z. Li, Y. Li, X. Chen, L. Zou, Y. Li, X. Yang, and H. Jiang, "Newsp: A new search process for continuous subgraph matching over dynamic graphs," in *ICDE*. IEEE, 2024, pp. 3324–3337.
[12] R. Yang, Z. Zhang, W. Zheng, and J. X. Yu, "Fast continuous subgraph matching over streaming graphs via backtracking reduction," *Proc. ACM Manag. Data*, vol. 1, no. 1, pp. 15:1–15:26, 2023.
[13] K. Kim, I. Seo, W. Han, J. Lee, S. Hong, H. Chafi, H. Shin, and G. Jeong, "Turboflux: A fast continuous subgraph matching system for streaming graph data," in *SIGMOD*, 2018, pp. 411–426.
[14] S. Min, S. G. Park, K. Park, D. Giammarresi, G. F. Italiano, and W. Han, "Symmetric continuous subgraph matching with bidirectional dynamic programming," *Proc. VLDB Endow.*, vol. 14, no. 8, pp. 1298–1310, 2021.
[15] K. Kim, I. Seo, W. Han, J. Lee, S. Hong, H. Chafi, H. Shin, and G. Jeong, "Turboflux: A fast continuous subgraph matching system for streaming graph data," in *SIGMOD*, 2018, pp. 411–426.
[16] X. Sun, S. Sun, Q. Luo, and B. He, "An in-depth study of continuous subgraph matching," *Proc. VLDB Endow.*, vol. 15, no. 7, pp. 1403–1416.
[17] V. Koibichuk, N. Ostrovska, F. Kashiyeva, and A. Kwilinski, "Innovation technology and cyber frauds risks of neobanks: gravity model analysis," *Marketing i menedžment innovacij*, no. 1, pp. 253–265, 2021.
[18] J. M. Karpoff, "The future of financial fraud," *Journal of Corporate Finance*, vol. 66, p. 101694, 2021.
[19] P. O. Shoetan and B. T. Familoni, "Transforming fintech fraud detection with advanced artificial intelligence algorithms," *Finance & Accounting Research Journal*, vol. 6, no. 4, pp. 602–625, 2024.
[20] J. Yang, S. Fang, Z. Gu, Z. Ma, X. Lin, and Z. Tian, "Tc-match: Fast time-constrained continuous subgraph matching," *Proc. VLDB Endow.*, vol. 17, no. 11, pp. 2791–2804, 2024.
[21] S. Choudhury, L. B. Holder, G. C. Jr., K. Agarwal, and J. Feo, "A selectivity based approach to continuous pattern detection in streaming graphs," in *EDBT*, 2015, pp. 157–168.
[22] K. Semertzidis and E. Pitoura, "A hybrid approach to temporal pattern matching," in *ASONAM*, 2020, pp. 384–388.
[23] I. W. Widnyana and S. R. Widyawati, "Role of forensic accounting in the diamond model relationship to detect the financial statement fraud," *International Journal of Research in Business and Social Science (2147-4478)*, vol. 11, no. 6, pp. 402–409, 2022.
[24] Y. Li, L. Zou, M. T. Özsu, and D. Zhao, "Time constrained continuous subgraph search over streaming graphs," in *ICDE*. IEEE, 2019, pp. 1082–1093.
[25] S. Min, J. Jang, K. Park, D. Giammarresi, G. F. Italiano, and W. Han, "Time-constrained continuous subgraph matching using temporal information for filtering and backtracking," in *ICDE*. IEEE, 2024, pp. 3257–3269.
[26] V. Bonnici, R. Giugno, A. Pulvirenti, D. E. Shasha, and A. Ferro, "A subgraph isomorphism algorithm and its application to biochemical data," *BMC Bioinform.*, vol. 14, no. S-7, p. S13, 2013.
[27] F. Bi, L. Chang, X. Lin, L. Qin, and W. Zhang, "Efficient subgraph matching by postponing cartesian products," in *SIGMOD*, 2016, pp. 1199–1214.
[28] F. Li, Z. Zou, and J. Li, "Durable subgraph matching on temporal graphs," *IEEE Trans. Knowl. Data Eng.*, vol. 35, no. 5, pp. 4713–4726, 2023.
[29] C. Kankanamge, S. Sahu, A. Mhedhbi, J. Chen, and S. Salihoglu, "Graphflow: An active graph database," in *SIGMOD*, 2017, pp. 1695–1698.
[30] S. Choudhury, L. B. Holder, G. C. Jr., K. Agarwal, and J. Feo, "A selectivity based approach to continuous pattern detection in streaming graphs," in *EDBT*, 2015, pp. 157–168.
[31] M. Idris, M. Ugarte, S. Vansummeren, H. Voigt, and W. Lehner, "General dynamic yannakakis: conjunctive queries with theta joins under updates," *VLDB J.*, vol. 29, no. 2-3, pp. 619–653, 2020.
[32] J. R. Ullmann, "An algorithm for subgraph isomorphism," *J. ACM*, vol. 23, no. 1, pp. 31–42, 1976.
[33] H. Kim, J. Lee, S. S. Bhowmick, W. Han, J. Lee, S. Ko, and M. H. A. Jarrah, "DUALSIM: parallel subgraph enumeration in a massive graph on a single machine," in *SIGMOD*, 2016, pp. 1231–1245.
[34] F. N. Afrati, D. Fotakis, and J. D. Ullman, "Enumerating subgraph instances using map-reduce," in *ICDE*, 2013, pp. 62–73.
[35] L. Lai, L. Qin, X. Lin, Y. Zhang, and L. Chang, "Scalable distributed subgraph enumeration," *Proc. VLDB Endow.*, vol. 10, no. 3, pp. 217–228, 2016.
[36] H. Kim, Y. Choi, K. Park, X. Lin, S. Hong, and W. Han, "Fast subgraph query processing and subgraph matching via static and dynamic equivalences," *VLDB J.*, vol. 32, no. 2, pp. 343–368, 2023.
[37] W. Guo, Y. Li, M. Sha, B. He, X. Xiao, and K. Tan, "Gpu-accelerated subgraph enumeration on partitioned graphs," in *SIGMOD*, 2020, pp. 1067–1082.
[38] F. Bi, L. Chang, X. Lin, L. Qin, and W. Zhang, "Efficient subgraph matching by postponing cartesian products," in *SIGMOD*, 2016, pp. 1199–1214.
[39] M. Han, H. Kim, G. Gu, K. Park, and W. Han, "Efficient subgraph matching: Harmonizing dynamic programming, adaptive matching order, and failing set together," in *SIGMOD*, 2019, pp. 1429–1446.
[40] A. Mhedhbi and S. Salihoglu, "Optimizing subgraph queries by combining binary and worst-case optimal joins," *Proc. VLDB Endow.*, vol. 12, no. 11, pp. 1692–1704, 2019.
[41] S. Bouhenni, S. Yahiaoui, N. Nouali-Taboudjemat, and H. Kheddouci, "A survey on distributed graph pattern matching in massive graphs," *ACM Comput. Surv.*, vol. 54, no. 2, pp. 36:1–36:35, 2022.
[42] P. Yuan, P. Liu, B. Wu, H. Jin, W. Zhang, and L. Liu, "Triplebit: a fast and compact system for large scale RDF data," *Proc. VLDB Endow.*, vol. 6, no. 7, pp. 517–528, 2013.
[43] H. Shang, Y. Zhang, X. Lin, and J. X. Yu, "Taming verification hardness: an efficient algorithm for testing subgraph isomorphism," *Proc. VLDB Endow.*, vol. 1, no. 1, pp. 364–375, 2008.
[44] A. Jüttner and P. Madarasi, "VF2++ - an improved subgraph isomorphism algorithm," *Discret. Appl. Math.*, vol. 242, pp. 69–81, 2018.
[45] S. Zhang, S. Li, and J. Yang, "GADDI: distance index based subgraph matching in biological networks," in *EDBT*, 2009, pp. 192–203.
[46] X. Jian, Z. Li, and L. Chen, "SUFF: accelerating subgraph matching with historical data," *Proc. VLDB Endow.*, vol. 16, no. 7, pp. 1699–1711, 2023.
[47] Z. Yang, L. Lai, X. Lin, K. Hao, and W. Zhang, "HUGE: an efficient and scalable subgraph enumeration system," in *SIGMOD*, 2021, pp. 2049–2062.
[48] T. Jin, B. Li, Y. Li, Q. Zhou, Q. Ma, Y. Zhao, H. Chen, and J. Cheng, "Circinus: Fast redundancy-reduced subgraph matching," *Proc. ACM Manag. Data*, vol. 1, no. 1, pp. 12:1–12:26, 2023.
[49] C. R. Rivero and H. M. Jamil, "Efficient and scalable labeled subgraph matching using sgmatch," *Knowl. Inf. Syst.*, vol. 51, no. 1, pp. 61–87, 2017.
[50] H. He and A. K. Singh, "Graphs-at-a-time: query language and access methods for graph databases," in *SIGMOD*, 2008, pp. 405–418.
[51] W. Han, J. Lee, and J. Lee, "Turbo$_{\text{ISO}}$: towards ultrafast and robust subgraph isomorphism search in large graph databases," in *SIGMOD*, 2013, pp. 337–348.
[52] G. Micale, G. Locicero, A. Pulvirenti, and A. Ferro, "Temporalri: subgraph isomorphism in temporal networks with multiple contacts," *Appl. Netw. Sci.*, vol. 6, no. 1, p. 55, 2021.
[53] P. Mackey, K. Porterfield, E. Fitzhenry, S. Choudhury, and G. C. Jr., "A chronological edge-driven approach to temporal subgraph isomorphism," in *IEEE*, 2018, pp. 3972–3979.
[54] Y. Ma, Y. Yuan, M. Liu, G. Wang, and Y. Wang, "Graph simulation on large scale temporal graphs," *GeoInformatica*, vol. 24, no. 1, pp. 199–220, 2020.
[55] F. Li and Z. Zou, "Subgraph matching on temporal graphs," *Inf. Sci.*, vol. 578, pp. 539–558, 2021.
[56] F. Li, Z. Zou, J. Li, X. Yang, and B. Wang, "Evolving subgraph matching on temporal graphs," *Knowl. Based Syst.*, vol. 258, p. 109961, 2022.

[57] N. Masuda and P. Holme, "Small inter-event times govern epidemic spreading on networks," *Physical Review Research*, vol. 2, no. 2, p. 023163, 2020.

[58] G. Locicero, G. Micale, A. Pulvirenti, and A. Ferro, "Temporalri: A subgraph isomorphism algorithm for temporal networks," in *Complex Networks*, 2020, pp. 675–687.

[59] A. Deutsch, N. Francis, A. Green, K. Hare, B. Li, L. Libkin, T. Lindaaker, V. Marsault, W. Martens, J. Michels, F. Murlak, S. Plantikow, P. Selmer, O. van Rest, H. Voigt, D. Vrgoc, M. Wu, and F. Zemke, "Graph pattern matching in GQL and SQL/PGQ," in *SIGMOD*, 2022, pp. 2246–2258.

[60] A. Aghasadeghi, J. V. den Bussche, and J. Stoyanovich, "Temporal graph patterns by timed automata," *VLDB J.*, vol. 33, no. 1, pp. 25–47, 2024.

[61] J. Giavitto and J. Echeveste, "Real-time matching of antescofo temporal patterns," in *International Symposium on Principles and Practice of Declarative Programming*, 2014, pp. 93–104.

[62] P. Liu, A. R. Benson, and M. Charikar, "Sampling methods for counting temporal motifs," in *WSDM*, 2019, pp. 294–302.

[63] X. Sun, Y. Tan, Q. Wu, B. Chen, and C. Shen, "Tm-miner: Tfs-based algorithm for mining temporal motifs in large temporal network," *IEEE Access*, vol. 7, pp. 49 778–49 789, 2019.

[64] A. Paranjape, A. R. Benson, and J. Leskovec, "Motifs in temporal networks," *CoRR*, vol. abs/1612.09259, 2016.

[65] A. Züfle, M. Renz, T. Emrich, and M. Franzke, "Pattern search in temporal social networks," in *EDBT*, 2018, pp. 289–300.

[66] C. Kosyfaki, N. Mamoulis, E. Pitoura, and P. Tsaparas, "Flow motifs in interaction networks," in *EDBT*, 2019, pp. 241–252.

[67] M. R. Henzinger, T. A. Henzinger, and P. W. Kopke, "Computing simulations on finite and infinite graphs," in *Annual Symposium on Foundations of Computer Science*, 1995, pp. 453–462.

[68] S. Gillani, G. Picard, and F. Laforest, "Continuous graph pattern matching over knowledge graph streams," in *DEBS*, 2016, pp. 214–225.

[69] T. Zhang, Y. Gao, L. Qiu, L. Chen, Q. Linghu, and S. Pu, "Distributed time-respecting flow graph pattern matching on temporal graphs," *World Wide Web*, vol. 23, no. 1, pp. 609–630, 2020.